Renormalization of chiral two-pion exchange NN interactions with Δ excitations: Central phases and the deuteron

M. Pavón Valderrama[1,*] and E. Ruiz Arriola[2,†]

[1]*Institut für Kernphysik and Jülich Center for Hadron Physics, Forschungszentrum Jülich, D-52425 Jülich, Germany*

[2]*Departamento de Física Atómica, Molecular y Nuclear, Universidad de Granada, E-18071 Granada, Spain*

(Received 16 October 2008; published 13 April 2009)

The renormalization of the chiral np interaction with Δ excitations in intermediate states is considered at next-to-leading order and next-to-next-to-leading order for central waves. The inclusion of the Δ excitation as an explicit degree of freedom improves the convergence properties of the effective field theory results for np scattering with respect to Δ-less theory and allows the existence of a deuteron bound state in the infinite cutoff limit. The $^1S_0$ singlet and $^3S_1$ triplet phase shifts reproduce data for $p \sim m_\pi$. The role of spectral function regularization is also discussed.

DOI: 10.1103/PhysRevC.79.044001 PACS number(s): 13.75.Cs, 03.65.Nk, 11.10.Gh, 21.30.Fe

I. INTRODUCTION

The nucleon-nucleon (NN) interaction problem has a well-deserved reputation of being a difficult one (for a review see, e.g., Ref. [1]). One obvious reason may be found in the theoretical and experimental inaccessibility of the shortest-distance interaction region relevant to nuclear physics. This lack of fundamental knowledge might be remedied in the future by *ab initio* lattice calculations, for which some incipient results already exist [2,3]. However, the current situation does not prevent us from addressing many facets of NN interactions, particularly long-distance features, provided short-distance insensitivity is guaranteed. Despite the great efforts during the years based on successful phenomenology [4–7], only during the past decade has the parentage to the underlying QCD been made more explicit after the proposal [8,9] to use effective field theory (EFT) methods and extensive use of chiral symmetry (for comprehensive reviews see, e.g., Refs. [10–12]). EFT starts out with the most general Lagrangian in terms of the relevant degrees of freedom compatible with chiral symmetry, dimensional analysis, and perturbative renormalization, organized by a prescribed power counting based on assuming a large-scale suppression on the parameters $4\pi f_\pi \sim M_N \sim 1$ GeV. Thus, by construction, EFT complies to the expectation of short-distance insensitivity, provided that enough counterterms encoding the unknown short-distance physics are added in perturbation theory to a finite order [9,13–20]. However, the physics of bound states, such as the deuteron, is genuinely nonperturbative and an infinite resummation of diagrams proves necessary (this does not necessarily involve the iteration of *all* diagrams; see, for example, Refs. [17,18], in which only the lowest-order contact interactions are resummed, or Ref. [21] for a new reformulation of the previous idea). There arises the problem of nonperturbative renormalization and/or modifications of the original power counting for which no universally accepted scheme has been found yet, mainly because the requirements may vary. Thus, although the EFT method does comply to model independence, it is far from trivial to achieve regulator independence and a converging pattern dictated by a reasonable power counting within a nonperturbative setup.

The NN renormalization problem may be cast efficiently in the traditional language of potentials and the corresponding Schrödinger equation. In addition to phrasing the NN interaction into the familiar and more intuitive nonrelativistic quantum mechanical framework, this procedure has also the advantage that the perturbative determination of the potential complies to the desired short-distance insensitivity for the potential itself [9,13–16,22]. The unconventional feature is that chiral expansions necessarily involve singular potentials at short distances, i.e., $r^2|V(r)| \to \infty$ for $r \to 0$. Indeed, in the limit $r \ll 1/m_\pi$ (or equivalently large momenta) pion mass effects are irrelevant in loop integrals and hence at some fixed order of the expansion one has for the coupled channel potential[1]

$$V(r) \to \frac{M_N \mathbf{c}_{2n+m+r}}{(4\pi f_\pi)^{2n} M_N^m \Delta^r} \frac{1}{r^{2n+m+r}}, \tag{1}$$

where n, m, and r are non-negative ($\geqslant 0$) integers, Δ the $N\Delta$ splitting, and $\mathbf{c}_k$, with $k = 2n + m + r$, is a dimensionless matrix of van der Waals coefficients in coupled-channels space. The dimensional argument is reproduced by loop calculations in the Weinberg dimensional power counting [9,13–16,22–24] and is scheme independent. It is thus conceivable that much of our understanding on the physics deduced from chiral potentials might be related to a proper interpretation of these highly singular potentials, which degree of singularity increases with the order of the expansion. This, of course, raises the question about in what sense higher-order potentials are smaller. One obvious way to ensure this desired smallness is by keeping a finite and sufficiently moderate cutoff [9,23–28], so the singularity of the potential is not probed, effectively recovering the power counting expectations for the size of higher-order contributions. The disadvantage is that results are strongly

*m.pavon.valderrama@fz-juelich.de

†earriola@ugr.es

[1]The only exception is the singlet channel one-pion-exchange (OPE) case that behaves as $\sim m_\pi^2/f_\pi^2 r$; see below.

cutoff dependent for scales about $r_c \sim 0.5$–1.0 fm, similar to the ones probed in NN scattering [29–32]. However, this is not the only possibility. Explicit computations [29–31] show that, when the cutoff is removed, the higher-order contributions will continue to generate only small changes in the amplitudes under specific circumstances that can be determined *a priori*. As emphasized in previous works [29–31], renormalization is the most natural tool provided (1) we expect the potential to be realistic at long distances and (2) we want short-distance details to be inessential in the description. As discussed above, this is precisely the situation we face most often in nuclear physics. A surprising and intriguing feature is that knowledge on the attractive or repulsive character of the singularity, i.e., the sign of the eigenvalues of $\mathbf{c}_k$ in Eq. (1), turns out to be crucial to successfully achieve this program and ultimately depends on the particular scheme or power counting used to compute the potential.

The singularities of chiral potentials may be disconcerting,[2] but they can be handled in a way that do not differ much from the standard treatment of well-behaved regular potentials that one usually encounters in nuclear physics [35]. Renormalization is the mathematical implementation of the appealing physical requirement of short-distance insensitivity and hence a convenient tool to search for typical long-distance model- and regulator independent results. In a nonperturbative setup such as the NN problem, renormalization imposes rather tight constraints on the interplay between the unknown short-distance physics and the perturbatively computable long-distance interactions [29–31]. This viewpoint provides useful insights and it is within such a framework that we envisage a systematic and model-independent description of the NN force based on chiral interactions. In this regard it is amazing to note how the sophisticated machinery of perturbative renormalization in quantum field theory used to compute the chiral potentials has not been so extensively developed when the inevitable nonperturbative physics must be incorporated; quite often the renormalization process is implemented by trial-and-error methods by adding counterterms suggested by the *a priori* power counting in momentum space. However, detailed analyses in coordinate and momentum space [29–31,36–38] show that the allowed structure of counterterms can be anticipated on purely analytical grounds and cannot be chosen independently on the long-distance potential (see also Refs. [39,40] for numerical work). Specifically, for a channel subspace with good total angular momentum the number of counterterms is $n(n+1)/2$, with n the number of negative eigenvalues of the van der Waals matrix $\mathbf{c}_k$ in Eq. (1). In fact, the much simpler coordinate space renormalization has been shown to be fully equivalent to the popular momentum space treatment for purely contact theories [41] and theories containing additional long range physics [42,43]. On the light of these latter studies the smallness of increasingly singular potentials such as Eq. (1) is triggered quite naturally by choosing the regular solution of the Schrödinger equation; the wave function behaves as $u_p(r) \sim (4\pi f_\pi r)^{\frac{2n+m+r}{4}}$ (modulo prefactors depending on the attractive or repulsive character of the potential). Thus, as shown in Ref. [43], when the short distance cutoff r_c approaches a *fixed scale*, $\sim 1/(4\pi f_\pi) = 0.2$ fm, an increasing $\mathcal{O}(r_c^{n+m/2+r/2+1})$ insensitivity of phase shifts and deuteron properties is guaranteed as the power of the singularity of the potential increases. Indeed, calculations with chiral two-pion exchange (TPE) potentials reproducing low-energy NN data display this insensitivity for reasonable scales of $r_c \sim 0.5$ fm [29,30] that correspond to the shortest wavelength probed by NN scattering in the elastic region. Within such a scenario, the discussion on whether one should remove the cutoff [29,30,32,44,45] would become less relevant as the order of the chiral expansion is increased in the computations. This requires of course that the same renormalization conditions are implemented for the computations to represent a specific physical situation and that the cutoff lies in the stability region $r_c \sim 0.5$ fm, which in turn means that renormalization has effectively been achieved.

However, despite all these findings, the question of how a sensible hierarchy for NN interactions should be organized has been left open. Although we know *whether* and, in the positive case, *how* this can be made compatible with the desired short-distance insensitivity [29–31], not all chiral potentials based on any given power counting are necessarily eligible. The Weinberg counting based in a heavy baryon approach at leading order (LO) [11] turns out to be renormalizable for the $^3S_1$-$^3D_1$ state [29] due to the attractive-repulsive character of the coupled-channels eigenpotentials at short distances; for the $^1S_0$ state it is again renormalizable, but at the price of including an additional, chiral-symmetry-breaking, higher-order counterterm [19]. There is at present no logical need why this ought to be so at higher orders, for the simple reason that power counting does not anticipate the sign of the interaction at short distances. In fact when one goes to next-to-leading order (NLO) the short distance $1/r^5$ singular repulsive character of the potential makes the deuteron unbound [30] because the interaction becomes singular and repulsive. Finally, next-to-next-to-leading order (NNLO) potentials diverge as $-1/r^6$ and are, again, compatible with Weinberg counting in the deuteron [30], in this case because the interaction is singular and attractive. Further inconsistencies between Weinberg's power counting and renormalization have been reported in Refs. [32,42]. The previous examples show clearly that the requirement of renormalizability can be in open conflict with the idea of a convergent pattern based on a preconceived chiral expansion and the mere dimensional power counting of the original proposal [8]. In particular, the assumption that the NN potential cannot be completely determined at arbitrary short distances is incompatible with a fully repulsive short distance singularity because finiteness implies that no counterterm is allowed.[3]

In this regard one should note an interesting analogy between the NN interaction in the chiral quark model (for a review, see, e.g., Refs. [46–48]) and the van der Waals molecular interactions in the Born-Oppenheimer approximation [30].

[2]Early treatments can be found in Ref. [33] (see Ref. [34] for an early review).

[3]In the coupled-channels case that means *all* eigenchannels are repulsive at short distances.

For nonrelativistic constituent quarks the NN interaction is provided by the convoluted OPE quark-quark potential in the direct channel because quark exchange and finite nucleon size effects can be neglected for distances larger than the nucleon size. Second-order perturbation theory in OPE among quarks generates TPE between nucleons yielding

$$V_{NN} = \langle NN|V_{\rm OPE}|NN\rangle + \sum_{HH'\neq NN} \frac{|\langle NN|V_{\rm OPE}|HH'\rangle|^2}{E_{NN}-E_{HH'}} + \cdots \tag{2}$$

for the NN potential, where $|NN\rangle$ represents a two-nucleon state and $|HH'\rangle$ an arbitrary intermediate state. In Regge theory one has the relation $M_\Delta^2 - M_N^2 = m_\rho^2 - m_\pi^2$ [49], m_ρ being the ρ mass, which in the chiral limit and for $M_N \sim N_c m_\rho/2$ implies a $N\Delta$ splitting $\Delta \sim m_\rho^2/2M_N \sim m_\rho/N_c = 256$ MeV for $N_c = 3$ and suggests a scale numerically comparable to twice the pion mass, which actually vanishes for $N_c \to \infty$. Thus, it makes sense to consider an EFT where the ΔN splitting is regarded as a small parameter [50,51]. Actually, when $HH' = N\Delta$ and $HH' = \Delta\Delta$, Eq. (2) resembles the result found using the Feynman graph technique [14]. Moreover, the second-order perturbative character suggests that the potential becomes attractive, because $E_{NN} - E_{N\Delta} = -\Delta$ and $E_{NN} - E_{\Delta\Delta} = -2\Delta$. At short distances the matrix elements scale as $\langle NN|V_{\rm OPE}|HH'\rangle \sim g_A^2/(f_\pi^2 r^3)$ and hence the potential becomes singular $\sim -g_A^4/(\Delta f_\pi^4 r^6)$ and attractive, necessarily being renormalizable with an arbitrary number of counterterms through energy-dependent boundary conditions [36]. Clearly, the renormalization of a potential where the $N\Delta$ splitting is treated as a small scale deserves further investigation because it appears as an obvious candidate where all necessary requirements for a convergent and short-distance insensitive scheme might be met. In the present article we check that the naive expectations based on the simple Eq. (2) are indeed verified for the long-distance chiral potentials including Δ degrees of freedom [9,13,14,52].

The Δ isobar has played a crucial role in the development of nuclear and particle physics (see, e.g., Refs. [53,54] and references therein). In addition to fixing the number of colours $N_c = 3$ in QCD to comply with the Pauli principle both at the quark as well as at the hadron level, this state can be clearly seen in πN scattering as a resonance, and it ubiquitously appears whenever the nucleon excitation energy is about the Δ-nucleon splitting, $\Delta = M_\Delta - M_N = 293$ MeV. Already in the earliest implementations of Weinberg's ideas the influence of Δ degrees of freedom was considered [9,55,56] in old-fashioned perturbation theory where energy-dependent potentials are generated. Energy-independent potentials have been obtained using the Feynman diagram technique a decade ago [13,14] and only recently the N2LO contributions have also been worked out in Ref. [52], where peripheral np phase shifts are computed in perturbation theory for these Δ contributions. Finite cutoff calculations involving Δ degrees of freedom to NLO have been analyzed in momentum space [25]. It has been shown that the inclusion of the Δ excitation improves the convergence of the chiral expansion of the NN interaction [57,58]. The renormalization of the $^1S_0$ phase with the NLO-Δ chiral potential has also been discussed recently in momentum space [42]. Short-distance insensitivity has also been discussed in other contexts different from NN collisions such as πd scattering at threshold [59] where a rationale for the multiple scattering expansion was indeed supported by the chiral singular potentials. Unfortunately, boost corrections being proportional to the average relative pn kinetic energy in the deuteron, $\langle p^2\rangle_d/M$, turned out to diverge due to the infinitely many short oscillations of the wave function. Recently, the benefits of including the Δ in such a process are discussed in Ref. [60] where it is shown how a proper reorganization of the boost corrections not only makes them finite but also numerically small after renormalization in harmony with phenomenological expectations. The drawback is a proliferation of low-energy constants when including the Δ, which can render the Δ-full theory impractical at higher orders. The implications of a Δ-based power counting for the three nucleon problem are analyzed in Refs. [57,58].

In the present article we focus our interest in the crucial role played by the Δ isobar in NN scattering in the elastic region from the point of view of renormalization of chiral nuclear forces and how it might solve a long-standing problem. In addition to an acceptable phenomenology in the s-wave phases we also show that precisely because of the built-in short-distance insensitivity and unlike previous calculations where the Δ degrees of freedom were absent, the deuteron is always bound up to N2LO-Δ, the highest order computed at present [52].

The article is organized as follows. In Sec. II we review the formalism as applied to the energy-independent potentials in a Δ-full theory [13,14,52]. In Sec. III we discuss the simpler $^1S_0$ channel, including either one or two counterterms by means of an energy-dependent boundary condition. We analyze the deuteron bound state and its properties in Sec. IV. Scattering states in the $^3S_1$-$^3D_1$ channel as well as the corresponding phase shifts are constructed by orthogonality to the deuteron and compared to the results obtained with the Nijmegen II potential [6], which has a χ^2 per datum near one and therefore can be considered as an alternative partial wave analysis, compatible with the original Nijmegen PWA [5]. The results found in this article are further compared to the Δ-less theory in Sec. V with previous results [30]. In Sec. VI we address the issue of the relevant scales entering the calculation as well as the role of missing effects such as relativistic, 3π contributions or vector-meson exchange calculations. We also reanalyze a regularization of the potential based on the spectral representation motivated by dispersion relations [26–28,52] and discuss its meaning on the light of the present approach. Finally in Sec. VII we recapitulate our results and draw our main conclusions.

II. FORMALISM

In the present article we use coordinate space renormalization by means of boundary conditions [29–31]. The equivalence to momentum space renormalization using counterterms for singular potentials is discussed thoroughly in Refs. [42,43]. We use the energy independent long-distance chiral potentials of Refs. [13,14,52], which are on-shell

equivalent to the energy-dependent potentials of Ref. [9]. We follow the convention of taking $1/M$ corrections as $\mathcal{O}(p^2)$, in agreement with the original argument from Ref. [61] as well as with the calculations of Refs. [9,28], and the computation of the N2LO-Δ potential of Ref. [52]. We note that this convention is not universal, and keeping the $1/M$ corrections as $\mathcal{O}(p)$ is also customary.[4] This convention has the consequence that at NLO-Δ and N2LO-Δ relativistic corrections are suppressed [52]. The final expressions for the potential are taken from Ref. [52].

We solve the coupled-channels (coupled in angular momentum) Schrödinger equation for the relative motion, which in compact notation reads,

$$\left[-\frac{\nabla^2}{M}+V_{NN}(\vec{x})\right]\Psi(\vec{x})=E_{\text{c.m.}}\,\Psi(\vec{x}), \tag{3}$$

where the spin and isospin indices have not been explicitly written; $M=2M_pM_n/(M_p+M_n)$ is twice the reduced proton-neutron mass. In coordinate space the potential can be written as

$$\begin{aligned}V_{NN}(\vec{x}) &= V_C(r)+\tau\, W_C(r)+\sigma\,[V_S(r)+\tau\, W_S(r)]\\ &\quad + S_{12}\,[V_T(r)+\tau\, W_T(r)]\,,\end{aligned} \tag{4}$$

where spin-orbit and quadratic spin-orbit terms have been ignored as they are not present in the NLO-Δ and N2LO-Δ potentials from Ref. [52]. The operators τ, σ, and S_{12} are given by

$$\begin{aligned}\tau &= \vec{\tau}_1\cdot\vec{\tau}_2 = 2t(t+1)-3,\\ \sigma &= \vec{\sigma}_1\cdot\vec{\sigma}_2 = 2s(s+1)-3,\\ S_{12} &= 3\,\vec{\sigma}_1\cdot\hat{r}\vec{\sigma}_2\cdot\hat{r}-\vec{\sigma}_1\cdot\vec{\sigma}_2,\end{aligned} \tag{5}$$

where $\vec{\tau}_{1(2)}$ and $\vec{\sigma}_{1(2)}$ represent the proton(neutron) isospin and spin operators; $\vec{\tau}_1\cdot\vec{\tau}_2$ and $\vec{\sigma}_1\cdot\vec{\sigma}_2$ are evaluated for total isospin $t=0,1$ and total spin $s=0,1$. Note that in Ref. [52] the potential is local and there are no relativistic mass corrections at N2LO-Δ. For states with good total angular momentum j and total spin $s=1$, the tensor operator reads

$$S_{12}^j=\begin{bmatrix}-\frac{2(j-1)}{2j+1} & 0 & \frac{6\sqrt{j(j+1)}}{2j+1}\\ 0 & 2 & 0\\ \frac{6\sqrt{j(j+1)}}{2j+1} & 0 & -\frac{2(j+2)}{2j+1}\end{bmatrix}, \tag{6}$$

where the matrix indices represent the orbital angular momentum $l=j-1,\,j,\,j+1$. For $s=0$ states the tensor operator vanishes, $S_{12}^j=0$. We note that Fermi-Dirac statistics implies $(-)^{l+s+t}=-1$.

A remarkable feature that happens at LO, NLO-Δ, and N2LO-Δ [9,13,14,52] is that the spin-orbit coupling vanishes, as well as any relativistic corrections. As a consequence, for a given isospin the potential can be diagonalized. The corresponding eigenpotentials depend just on the isospin of the channel and not on the total angular momentum j. All the j dependence goes into the matrix that diagonalizes the potential. This can be seen in the following formulas:

$$\begin{aligned}\mathbf{V}^{1j} &= (V_C+\tau W_C)-3\,(V_S+W_S\tau)+S_{12}^j\,(V_T+\tau W_T)\\ &= M_j\ \text{diag}\,(A-4B,\,A+2B,\,A+2B)\ M_j^{-1},\end{aligned} \tag{7}$$

where $\mathbf{V}^{1j}$ is the triplet-channel potential written in matrix form, with

$$\begin{aligned}A &= (V_C+\tau W_C)-3\,(V_S+W_S\tau),\\ B &= (V_T+\tau W_T),\\ M_j &= \begin{pmatrix}\cos\theta_j & 0 & -\sin\theta_j\\ 0 & 1 & 0\\ \sin\theta_j & 0 & \cos\theta_j\end{pmatrix},\end{aligned} \tag{8}$$

where

$$\cos\theta_j=\sqrt{\frac{j}{2j+1}}. \tag{9}$$

The transformation M_j diagonalizes the full potential but *not* the Schrödinger equation, because it contains in addition to the potential the centrifugal barrier, which is a diagonal operator in the jls basis but does not remain diagonal in the rotated basis. Specific knowledge of the short-distance behavior is needed to carry on with the renormalization program. Generally, on purely dimensional grounds, we have for $r\to 0$

$$V_i(r)\to\frac{C_k^{V,i}}{r^k},\qquad W_i(r)\to\frac{C_k^{W,i}}{r^k}, \tag{10}$$

where

$$C^i_{k=2n+m+r+1}\sim\frac{1}{f_\pi^{2n}M_N^m\Delta^r}, \tag{11}$$

with Δ the $N\Delta$ splitting and n, m, and r non-negative integers. At short distances, the angular-momentum dependence may be neglected when the index $k>2$. The relevant issue to carry out the renormalization procedure and to generate finite results is to know whether the interaction is attractive or repulsive. It turns out that both NLO-Δ and N2LO-Δ potentials have a leading singularity behavior of $1/r^6$. In Appendix we list the analytical expressions for the van der Waals coefficients C_k^i, for $k=6$ (i.e., the leading singularity of the potential).

In our numerical calculations we take $f_\pi=92.4$ MeV, $m_\pi=138.03$ MeV, $2\mu_{np}=M_N=2M_pM_n/(M_p+M_n)=938.918$ MeV, $g_A=1.29$ in the OPE piece to account for the Goldberger-Treimann discrepancy and $g_A=1.26$ in the TPE piece of the potential.[5] The corresponding pion nucleon coupling constant takes then the value $g_{\pi NN}=13.083$ for the OPE piece of the potential. We use the ΔN splitting $\Delta=293$ MeV. For h_A and the low-energy constants c_1, c_2, c_3, c_4, b_3, and b_8 we take the values from Fits 1 and 2 of Ref. [52] (Table I

[4] Although the effect of keeping or ignoring the mass corrections is indeed small (see end of this section).

[5] Strictly speaking $g_A=1.26$ both in the OPE and TPE pieces of the potential, but it happens that at NLO and higher orders the OPE piece receives a contribution from the d_{18} LEC, related to the Goldberger-Treimann discrepancy, see, for example, the expressions of Ref. [26] for details. This is equivalent to consider the original expression for the OPE potential, but taking $g_A=1.29$ instead of $g_A=1.26$.

TABLE I. van der Waals MC_6 coefficients (in fm^4) for the different spin-isospin components of the NLO-Δ and N2LO-Δ potentials. We use the πN motivated Fits 1 and 2 of Ref. [52]. Fit 1 involves the SU(4) quark-model relation $h_A = 3g_A/(2\sqrt{2}) = 1.34$ for $g_A = 1.26$.

	$MC_{6,V,C}^{\text{NLO-}\Delta}$	$MC_{6,W,C}^{\text{NLO-}\Delta}$	$MC_{6,V,S}^{\text{NLO-}\Delta}$	$MC_{6,W,S}^{\text{NLO-}\Delta}$	$MC_{6,V,T}^{\text{NLO-}\Delta}$	$MC_{6,W,T}^{\text{NLO-}\Delta}$
Fit 1	−7.233	−1.201	0.601	0.301	−0.601	−0.301
Fit 2	−3.867	−0.833	0.417	0.177	−0.417	−0.177
	$MC_{6,V,C}^{\text{N2LO-}\Delta}$	$MC_{6,W,C}^{\text{N2LO-}\Delta}$	$MC_{6,V,S}^{\text{N2LO-}\Delta}$	$MC_{6,W,S}^{\text{N2LO-}\Delta}$	$MC_{6,V,T}^{\text{N2LO-}\Delta}$	$MC_{6,W,T}^{\text{N2LO-}\Delta}$
Fit 1	−1.241	−0.489	0.244	0.351	−0.244	−0.351
Fit 2	−4.381	−1.121	0.561	0.439	−0.561	−0.439

within that reference), where they are deduced from a fit to πN threshold parameters in S and P waves to the data of Ref. [62]. These values are compatible with all πN threshold parameters except $b_{0,+}^-$ that is about twice its recommended value [62] at this level of approximation. Fit 1 uses the SU(4) quark-model relation $h_A = 3\,g_A/2\sqrt{2}\,(= 1.34\,\text{for}\,g_A = 1.26)$, while Fit 2 uses $h_A = 1.05$.

The numerical values of the van der Waals coefficients MC_6 are summarized in Table I for the different components of the NLO-Δ and N2LO-Δ potentials. The van der Waals coefficients are additive: therefore one can obtain the coefficient corresponding to some given partial wave by adding the individual contributions, i.e.

$$\begin{aligned} MC_6 = {} & MC_{6,V,C}(r) + \tau\, MC_{6,W,C} \\ & + \sigma(MC_{6,V,S} + \tau\, MC_{6,W,S}) \\ & + S_{12}(MC_{6,V,T} + \tau\, MC_{6,W,T}). \end{aligned} \tag{12}$$

This is done for the singlet $^1S_0$ and the triplet $^3S_1$-$^3D_1$ channels in Table II.

We also present N2LO-$\not\Delta$ results for comparison purposes. For them we use the same parameters as in the N2LO-Δ computation, except for the c_1, c_3, and c_4 LECs, for which we use the following two different determinations: the so-called set IV of Ref. [30], which was obtained in Ref. [24] by fitting to NN scattering data, and the values from Ref. [52] for N2LO-$\not\Delta$ that we refer to as set πN and allow a better comparison with the N2LO-Δ computations presented here, as they are also fitted to reproduce πN S- and P-wave threshold parameters. Due to the different fitting procedures, any direct comparison between the results of Ref. [30], i.e., set IV, and the N2LO-Δ results should be done with care. It should be mentioned too that the results of Ref. [30] contain $1/M$ corrections to the potential. These corrections are nevertheless small and, if excluded, would induce only small differences in the results of Ref. [30].[6]

III. THE SINGLET CHANNEL

A. Equations and boundary conditions

The $^1S_0$ wave function in the pn center-of-mass (c.m.) system can be written as

$$\Psi(\vec{x}) = \frac{1}{\sqrt{4\pi}r} u(r) \chi_{pn}^{sm_s}, \tag{13}$$

with the total spin $s = 0$ and $m_s = 0$. The function $u(r)$ is the reduced S-wave function and satisfies the following reduced Schrödinger equation

$$-u_k''(r) + U_{^1S_0}(r) u_k(r) = k^2 u_k(r), \tag{14}$$

where k is the center-of-mass momentum and $U_{^1S_0}$ the reduced potential defined as

$$U_{^1S_0}(r) = M[V_C(r) + W_C(r) - 3V_S(r) - 3W_S(r)]. \tag{15}$$

For a finite energy-scattering state we solve for the chiral potential with the asymptotic normalization

$$u_k(r) \to \frac{\sin[kr + \delta_0(k)]}{\sin\delta_0(k)}, \tag{16}$$

with $\delta_0(k)$ the phase shift. For a potential falling off exponentially $\sim e^{-m_\pi r}$ at large distances, we have the effective range expansion, valid for momenta $|k| < m_\pi/2$,

$$k\cot\delta_0(k) = -\frac{1}{\alpha_0} + \frac{1}{2} r_0 k^2 + v_2 k^4 + \cdots \tag{17}$$

with α_0 the scattering length and r_0 the effective range. At short distances the NN chiral potential behaves as

$$U_{^1S_0}(r) \to \frac{MC_{6,^1S_0}}{r^6} = -\frac{R^4}{r^6}, \tag{18}$$

where

$$MC_{6,^1S_0} = MC_{6,^1S_0}^{\text{NLO-}\Delta} + MC_{6,^1S_0}^{\text{N2LO-}\Delta}, \tag{19}$$

which is a van der Waals-type interaction.[7] The numerical values for $MC_{6,^1S_0}^{\text{NLO-}\Delta}$ and $MC_{6,^1S_0}^{\text{N2LO-}\Delta}$ are listed in Table II. The value of the coefficient is negative, with the typical length scale $R = (-MC_6)^{1/4}$. The solution at short distances is of

[6] As an illustration, ignoring the $1/M$ corrections will yield to the following modifications for the results of Ref. [30] (original results in parentheses): $A_S = 0.887(0.884)$ fm$^{1/2}$, $r_m = 1.972(1.967)$ fm, $Q_d = 0.278(0.276)$ fm^2, $P_D = 8(8)\,\%$, $\langle r^{-1}\rangle = 0.442(0.447)$ fm^{-1}, $\langle r^{-2}\rangle = 0.276(0.284)$ fm^{-2}.

[7] It should be noted that the NLO-$\not\Delta$ potential is less singular than the NLO-Δ one at short distances, diverging as $1/r^5$ only.

TABLE II. van der Waals MC_6 coefficients (in fm^4) in the $^1S_0$ and $^3S_1$-$^3D_1$ (deuteron) channels of the NLO-Δ and N2LO-Δ potentials. We also present the corresponding negative eigenvalues $-R_+^4$ and $-R_-^4$ in the deuteron channel case. We use the πN motivated Fits 1 and 2 of Ref. [52]. Fit 1 involves the SU(4) quark-model relation $h_A = 3g_A/(2\sqrt{2}) = 1.34$ for $g_A = 1.26$.

	$MC^{\text{NLO-}\Delta}_{6,^1S_0}$	$MC^{\text{NLO-}\Delta}_{6,^3S_1}$	$MC^{\text{NLO-}\Delta}_{6,E_1}$	$MC^{\text{NLO-}\Delta}_{6,^3D_1}$	$-R_+^4$	$-R_-^4$
Fit 1	−11.138	−3.932	0.855	−4.537	−5.141	−3.327
Fit 2	−6.481	−1.482	0.322	−1.710	−1.938	−1.254
	$MC^{\text{N2LO-}\Delta}_{6,^1S_0}$	$MC^{\text{N2LO-}\Delta}_{6,^3S_1}$	$MC^{\text{N2LO-}\Delta}_{6,E_1}$	$MC^{\text{N2LO-}\Delta}_{6,^3D_1}$	$-R_+^4$	$-R_-^4$
Fit 1	−3.519	−0.585	2.290	−2.204	−3.823	1.035
Fit 2	−8.500	−1.773	2.138	−3.284	−4.796	−0.261

oscillatory type:

$$u_k(r) \to A\left(\frac{r}{R}\right)^{3/2} \sin\left[\frac{1}{2}\left(\frac{R}{r}\right)^2 + \varphi\right], \tag{20}$$

where A is a normalization constant and φ an undetermined phase, which may in principle depend on energy.

We will present below two calculations. In the first one the renormalization is carried out with one counterterm, which in turn means one renormalization condition. In such a case the short-distance phase becomes energy independent and orthogonality conditions are satisfied. In the second calculation we proceed with two counterterms, i.e., two renormalization conditions, for which the short-distance phase acquires a very specific energy dependence.

B. Renormalization with one counterterm

As mentioned, the phase shift is determined from Eq. (16), but to fix the undetermined phase φ we impose orthogonality for $r > r_c$ between the zero energy state and the state with momentum p. As shown in Ref. [30], orthogonality turns out to be equivalent to the following condition between 0- and k-momentum reduced wave functions at $r = r_c$

$$u_k'(r_c)u_0(r_c) - u_0'(r_c)u_k(r_c) = 0. \tag{21}$$

Taking the limit $r_c \to 0$ implies that the short-distance phase φ is energy independent [30]. Thus, for the zero energy state we solve

$$-u_0''(r) + U_{^1S_0}(r)u_0(r) = 0, \tag{22}$$

with the asymptotic normalization at large distances

$$u_0(r) \to 1 - \frac{r}{\alpha_0}, \tag{23}$$

where α_0 is the scattering length. In this equation α_0 is an input, so one needs to integrate Eq. (22) from infinity to the origin (in contrast with the usual procedure of integrating from the origin to infinity). The effective range, defined as

$$r_0 = 2\int_0^\infty dr\left[\left(1 - \frac{r}{\alpha_0}\right)^2 - u_0(r)^2\right], \tag{24}$$

can be computed. Due to the superposition principle, we can write the zero-momentum wave function as the following linear combination

$$u_0(r) = u_{0,c}(r) - \frac{1}{\alpha_0}u_{0,s}(r), \tag{25}$$

where $u_{0,c}(r) \to 1$ and $u_{0,s}(r) \to r$ correspond to cases where the scattering length is either infinity or zero, respectively. Using this decomposition, we get

$$r_0 = A + \frac{B}{\alpha_0} + \frac{C}{\alpha_0^2}, \tag{26}$$

where A, B, and C, defined as

$$A = 2\int_0^\infty dr\left(1 - u_{0,c}^2\right), \tag{27}$$

$$B = -4\int_0^\infty dr(r - u_{0,c}u_{0,s}), \tag{28}$$

$$C = 2\int_0^\infty dr\left(r^2 - u_{0,s}^2\right), \tag{29}$$

depend on the potential parameters only. The interesting thing is that all dependence on the scattering length α_0 is displayed explicitly by Eq. (26). Numerically we get

$$\begin{aligned}
r_0 &= 2.661 - \frac{5.707}{\alpha_0} + \frac{5.988}{\alpha_0^2} \quad (\text{NLO-}\Delta, h_A = 1.34),\\
r_0 &= 2.517 - \frac{5.430}{\alpha_0} + \frac{5.811}{\alpha_0^2} \quad (\text{NLO-}\Delta, h_A = 1.05),\\
r_0 &= 2.789 - \frac{5.992}{\alpha_0} + \frac{6.187}{\alpha_0^2} \quad (\text{N2LO-}\Delta,\ \text{Fit 1}),\\
r_0 &= 2.780 - \frac{5.969}{\alpha_0} + \frac{6.171}{\alpha_0^2} \quad (\text{N2LO-}\Delta,\ \text{Fit 2}).
\end{aligned} \tag{30}$$

The corresponding numerical values when the experimental $\alpha_0 = -23.74$ fm is taken, as well as the v_2 parameter can be looked up in Table III. As can be seen, the value of the effective range has a clear convergence pattern when going from LO to N2LO-Δ. The contribution coming from N2LO-Δ is very small compared to the NLO-Δ contribution, in agreement with the findings of Ref. [52]. This is in contrast with the Δ-less theory, for which N2LO generates a great correction over the NLO results. Unfortunately, the N2LO-Δ results converge to wrong values, about 3 fm for both Fits 1 and 2. The same happens for the N2LO-$\not\Delta$ results, although with a

TABLE III. Predicted threshold parameters in the singlet $^1S_0$ channel with one counterterm for Fits 1 and 2 of Ref. [52]. We compare our renormalized results given by the cutoff-independent universal formula (26) for r_0 and its extension for v_2 to finite cutoff NN calculations using their scattering length as an input. The experimental values for the scattering length and effective range are taken from Ref. [7].

	Calculation	α_0 (fm)	r_0 (fm)	v_2 (fm^3)
LO	Ref. [30]	Input	1.44	−2.11
NLO-$\not\Delta$	Ref. [30]	Input	2.29	−1.02
NLO-Δ ($h_A = 1.34$)	This work	Input	2.91	−0.32
NLO-Δ ($h_A = 1.05$)	This work	Input	2.76	−0.53
N2LO-$\not\Delta$ (Set IV)	Ref. [30]	Input	2.87	−0.38
N2LO-$\not\Delta$ (πN)	This work	Input	2.92	−0.31
N2LO-Δ (Fit 1)	This work	Input	3.05	−0.12
N2LO-Δ (Fit 2)	This work	Input	3.04	−0.13
Nijm II	Refs. [5,6]	−23.73	2.67	−0.48
Reid 93	Refs. [5,6]	−23.74	2.75	−0.49
Exp.	–	−23.74(2)	2.77(5)	–

weaker convergence pattern. The reason for this discrepancy is that the NLO and N2LO potentials, both in Δ-less and Δ-full theories, are too attractive at intermediate distances, thus yielding a bigger value for r_0 than the one obtained with phenomenological potentials like Nijmegen II or Reid93 [30,42].

Using the orthogonality condition, Eq. (21), the phase shift can be determined from the scattering length and the potential as independent parameters when the limit $r_c \to 0$ is taken. The renormalized phase shift is presented in Fig. 1 (left). The phase shifts are compared with the ones obtained from the Nijmegen II potential [6], which are compatible with the Nijmegen PWA [5]. As we see the trend in the effective range r_0 and the v_2 parameter is reflected in the behavior of the phase shift. In Ref. [42] a similar calculation was carried out in momentum space with inclusion of Δ degrees of freedom at NLO and one counterterm. The present NLO-Δ coordinate space results agree with that calculation when the SU(4) relation, $h_A = 1.34$, is used. As discussed in the previous paragraph for the effective range parameters, at N2LO-Δ the phase shifts have already converged, although to the wrong value, due to the excessive strength of the intermediate range of the potential. In the next section we will see how the situation changes when an extra counterterm is included in the computations. This counterterm will be fitted to reproduce the effective range.

C. Renormalization with two counterterms

In the standard Weinberg counting both the long-distance potential as well as the short-distance potential are

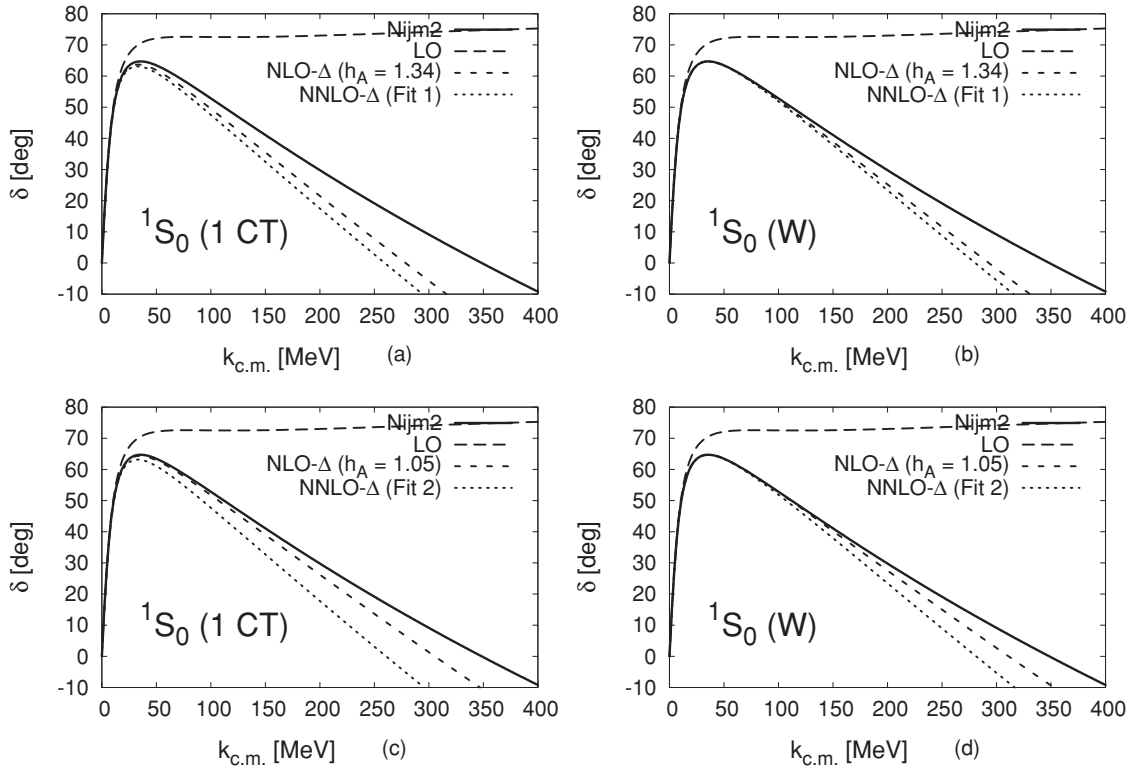

FIG. 1. Renormalized phase shifts for the LO, NLO-Δ, and N2LO-Δ potentials as a function of the center-of-mass np momentum $k_{\rm c.m.}$ in the $^1S_0$ singlet channel, compared to the Nijmegen II potential results [6]. The computations are done both with $h_A = 1.34$ (upper panels) and with $h_A = 1.05$ (lower panels). For the LO result, the calculation is always done with one counterterm, while for the NLO and N2LO results, computations are done with one counterterm (left panels) and two counterterms (right panels), corresponding in this last case to the standard Weinberg counting for the $^1S_0$ channel.

dimensionally expanded in momentum space. For the short-range piece, one writes $V_S(p', p) = C_0 + C_2(p^2 + p'^2) + \cdots$, where C_0, C_2, etc., are referred to as counterterms. In Ref. [42] the interrelation between the counterterms and short-distance boundary conditions in coordinate space has been discussed at length. At LO in the Weinberg counting one has only one counterterm. This corresponds to the situation described in the previous section. At NLO and N2LO in the Weinberg counting (both in the Δ-less and Δ-full cases), one adds two counterterms C_0 and C_2 for a fixed momentum space cutoff Λ, which may be fixed by reproducing the scattering length α_0 and the effective range r_0. The interesting finding was that such a procedure *does not* generate a converging $^1S_0$ phase shift in the limit $\Lambda \to \infty$ [42]. Thus, the momentum space polynomial parametrization of Weinberg counting is not compatible with renormalization. However, this does not necessarily mean that one cannot impose two renormalization conditions to fix the scattering length and the effective range. Actually, on a wider perspective one may pose on the one hand the problem of obtaining a finite phase shift embodying the chiral potential and on the other the problem of fixing both α_0 and r_0 as *independent* parameters. Fortunately, there exists a unique procedure in coordinate space [36] meeting the two previous conditions and yielding convergent phase shifts, which we apply below to discuss the $^1S_0$ channel when two counterterms are considered for NLO-Δ and N2LO-Δ chiral potentials. We will refer to this scheme as Weinberg counting with Δ.

The equivalent coordinate space procedure [36,42] consists of expanding the wave function in powers of the energy

$$u_k(r) = u_0(r) + k^2 u_2(r) + \cdots \tag{31}$$

where $u_0(r)$ and $u_2(r)$ satisfy the following equations:

$$-u_0''(r) + U_{^1S_0}(r)u_0(r) = 0, \tag{32}$$

$$\begin{aligned} u_0(r) &\overset{r\to\infty}{\to} 1 - \frac{r}{\alpha_0}, \\ -u_2''(r) + U_{^1S_0}(r)u_2(r) &= u_0(r), \\ u_2(r) &\overset{r\to\infty}{\to} \frac{\left(r^3 - 3\alpha_0 r^2 + 3\alpha_0 r_0 r\right)}{6\alpha_0}. \end{aligned} \tag{33}$$

The asymptotic conditions correspond to fixing α_0 and r_0 as independent parameters (two counterterms). The matching condition at the boundary $r = r_c$ becomes energy dependent [36]

$$\frac{u_k'(r_c)}{u_k(r_c)} = \frac{u_0'(r_c) + k^2 u_2'(r_c) + \cdots}{u_0(r_c) + k^2 u_2(r_c) + \cdots}, \tag{34}$$

whence the corresponding phase shift may be deduced by integrating in Eq. (32) and Eq. (33) and integrating out Eq. (14) with Eq. (16). It is worth mentioning that the energy-dependent matching condition, Eq. (34), is quite unique because this is the only representation for the boundary condition guaranteeing the existence of the limit $r_c \to 0$ for singular potentials [36]. As pointed out in Refs. [36,42], polynomial expansions in k^2 such as suggested, e.g., in the Nijmegen PWA [5] and implemented later on for chiral TPE potentials [16], do not work for $r_c \to 0$ and in fact generate undesired oscillations for $r_c \ll 1.4$ fm in the phase shifts. The validity of these features can be deduced analytically in coordinate space as a consequence of the RG invariance of a Moebius bilinear transformation [36]. Equivalent parametrizations in momentum space may likely exist but are so far unknown. As already mentioned, the widely used polynomial representation of short-distance interactions in momentum space $V_S(p', p) = C_0 + C_2(p^2 + p'^2) + \cdots$ of standard NLO and NNLO Weinberg counting implies that for $\Lambda \to \infty$ either C_2 is irrelevant when only α_0 is kept fixed or the phase shift does not converge when both α_0 and r_0 are simultaneously fixed [36,42].

In Figs. 1(a) and 1(b) we show the results for the two counterterm renormalized phase shifts at NLO-Δ and N2LO-Δ. As we see, the second counterterm is responsible for a certain improvement all over the elastic region, in particular in the region $k < m_\pi$ where TPE effects are expected to dominate in the singlet $^1S_0$-channel.[8]

At higher momenta, however, the discrepancy with the Nijmegen II potential results [6] and therefore with the Nijmegen PWA [5] persists. The second counterterm is therefore unable to provide the necessary repulsion to compensate for the excessive intermediate-range attraction present in the NLO-Δ and N2LO-Δ potentials. This result agrees with the findings of Ref. [42] and extends them from NLO-Δ to N2LO-Δ. Possible solutions to this disturbing situation include finite cutoff computations, which help to increase the effect of the second counterterm, and the inclusion of spectral function regularization, proposed in Ref. [26] precisely to treat the problem of the intermediate strength of the N2LO-$\not\Delta$ potential in peripheral partial waves. The case of spectral function regularization will be discussed in Sec. VI.

IV. THE TRIPLET CHANNEL

A. Equations and boundary conditions

The $^3S_1$-$^3D_1$ wave function in the pn center-of-mass system can be written as

$$\Psi(\vec{x}) = \frac{1}{\sqrt{4\pi}\, r}\left[u(r)\sigma_p \cdot \sigma_n + \frac{w(r)}{\sqrt{8}}(3\sigma_p \cdot \hat{x}\sigma_n \cdot \hat{x} - \sigma_p \cdot \sigma_n)\right]\chi_{pn}^{sm_s}, \tag{35}$$

with total spin $s = 1$ and $m_s = 0, \pm 1$; σ_p and σ_n are the Pauli matrices for the proton and the neutron, respectively. The functions $u(r)$ and $w(r)$ are the reduced S- and D-wave components of the relative wave function, respectively. They satisfy the coupled set of equations in the $^3S_1$-$^3D_1$ channel

$$\begin{aligned} -u''(r) + U_{^3S_1}(r)u(r) + U_{E_1}(r)w(r) &= k^2 u(r), \\ -w''(r) + U_{E_1}(r)u(r) + \left[U_{^3D_1}(r) + \frac{6}{r^2}\right]w(r) &= k^2 w(r), \end{aligned} \tag{36}$$

[8] In principle for $k < m_\pi$ OPE (instead of TPE) effects should dominate, but in the case of the $^1S_0$ singlet channel this is not the case due to the weakness of OPE in this channel. This happens only in the singlet channel; in the case of the triplet channel we recover the naive expectations, and OPE clearly dominates for $k < m_\pi$.

with $U_{^3S_1}(r)$, $U_{E_1}(r)$, and $U_{^3D_1}(r)$ the corresponding matrix elements of the coupled-channels potential, which are

$$\begin{aligned} U_{^3S_1} &= V_C - 3W_C + V_S - 3W_S, \\ U_{E_1} &= 2\sqrt{2}(V_T - 3W_T), \\ U_{^3D_1} &= V_C - 3W_C + V_S - 3W_S - 2V_T + 6W_T. \end{aligned} \tag{37}$$

At short distances one has

$$\begin{aligned} U_{^3S_1} &\to \frac{MC_{6,^3S_1}}{r^6}, \\ U_{E_1} &\to \frac{MC_{6,E_1}}{r^6}, \\ U_{^3D_1} &\to \frac{MC_{6,^3D_1}}{r^6}, \end{aligned} \tag{38}$$

where the van der Waals coefficients are given by

$$\begin{aligned} C_{6,^3S_1} &= C^{\rm NLO}_{6,^3S_1} + C^{\rm N2LO}_{6,^3S_1}, \\ C_{6,E_1} &= C^{\rm NLO}_{6,E_1} + C^{\rm N2LO}_{6,E_1}, \\ C_{6,^3D_1} &= C^{\rm NLO}_{6,^3D_1} + C^{\rm N2LO}_{6,^3D_1}. \end{aligned} \tag{39}$$

Their numerical values are listed in Table II for Fits 1 and 2 of Ref. [52]. One can diagonalize the corresponding matrix of van der Waals coefficients

$$\begin{pmatrix} MC_{6,^3S_1} & MC_{6,E_1} \\ MC_{6,E_1} & MC_{6,^3D_1} \end{pmatrix} = \begin{pmatrix} \cos\theta & \sin\theta \\ -\sin\theta & \cos\theta \end{pmatrix} \begin{pmatrix} -R_+^4 & 0 \\ 0 & -R_-^4 \end{pmatrix} \times \begin{pmatrix} \cos\theta & -\sin\theta \\ \sin\theta & \cos\theta \end{pmatrix}, \tag{40}$$

where, according to Eq. (9), the angle is

$$\cos\theta = \frac{1}{\sqrt{3}}, \tag{41}$$

i.e., $\theta = 54.7^\circ$ and common to both the NLO-Δ and N2LO-Δ potentials. That means that the eigenvalues of the NLO-Δ and N2LO-Δ van der Waals matrices are additive and therefore can be summed up directly from Table II:

$$-R_\pm^4 = -R_{\pm,\rm NLO}^4 - R_{\pm,\rm N2LO}^4. \tag{42}$$

As we see from Table II, the NLO-Δ matrix is negative definite, but the N2LO-Δ matrix is not so for Fit 1. However, what counts is the NLO-Δ + N2LO-Δ contribution that, as can be checked, is negative definite. In the diagonal basis one has at short distances

$$\begin{pmatrix} u \\ w \end{pmatrix} \to \begin{pmatrix} \cos\theta & \sin\theta \\ -\sin\theta & \cos\theta \end{pmatrix} \begin{pmatrix} v_+ \\ v_- \end{pmatrix}, \tag{43}$$

where the short-distance eigenfunctions are

$$\begin{aligned} v_+(r) &= \left(\frac{r}{R_+}\right)^{\frac{3}{2}} C_+ \sin\left[\frac{1}{2}\frac{R_+^2}{r^2} + \varphi_+\right] \\ v_-(r) &= \left(\frac{r}{R_-}\right)^{\frac{3}{2}} C_- \sin\left[\frac{1}{2}\frac{R_-^2}{r^2} + \varphi_-\right], \end{aligned} \tag{44}$$

and $\varphi_\pm$ are short-distance phases that must be fixed independently on the potential and $C_\pm$ suitable normalization constants. Orthogonality of solutions of different energy requires these phases to be energy independent. Following the procedure of Ref. [30] we fix them from deuteron physical properties, namely the binding energy and asymptotic D/S ratio (see below). Once these two quantities are fixed, scattering states can be completely determined by fixing in addition the scattering length of the $^3S_1$ phase and then imposing orthogonality to the deuteron state. This is equivalent to renormalizing with three counterterms in momentum space [43]. Of course, more counterterms could be considered if orthogonality is given up by an energy-dependent boundary condition, as done above for the $^1S_0$ channel.

In the following two subsections we will consider the description of the deuteron bound state and the scattering states and discuss our results.

B. The deuteron

In the case of negative energy we consider Eq. (36) with

$$k^2 = -\gamma^2 = -M\,B_d, \tag{45}$$

with γ the deuteron wave number and B_d the deuteron binding energy. We solve Eq. (36) together with the asymptotic condition at infinity

$$\begin{aligned} u(r) &\to A_S e^{-\gamma r}, \\ w(r) &\to A_D e^{-\gamma r}\left[1 + \frac{3}{\gamma r} + \frac{3}{(\gamma r)^2}\right], \end{aligned} \tag{46}$$

where A_S and A_D are the S- and D-wave normalization factors. The asymptotic D/S ratio parameter η is defined as $\eta = A_D/A_S$.

To obtain the regularized wave functions, we fix γ and η to their experimental values (see Table IV) and obtain $u(r)$ and $w(r)$ by integrating Eq. (36) from $r \to \infty$ to $r = 0$ with (46) as boundary conditions. A_S can be later determined from

$$\int_0^\infty dr\,[u(r)^2 + w(r)^2] = 1, \tag{47}$$

i.e., from demanding the deuteron normalization to be equal to unity. The renormalized deuteron wave functions are depicted in Fig. 2 at LO, NLO-Δ, and N2LO-Δ and compared to the Nijmegen II wave functions [6]. The asymptotic normalization $u \to e^{-\gamma r}$ has been adopted and the asymptotic D/S ratio is taken to be $\eta = 0.0256$. One can see in Fig. 2 the appearance of an increasing number of oscillations in the wave function when the radius approaches zero. They have no appreciable effect on the physics of the deuteron, as they happen at very short distances. Therefore they have a very small effect on the computation of deuteron observables and cannot be resolved by external probes at the energies for which the effective theory description is valid. This later point is shown explicitly in Ref. [43] for elastic electron-deuteron scattering. Perhaps the most remarkable aspect of the present calculation is the convergence of the proposed scheme when the Δ resonance is considered, which of course implies that the deuteron is bound at all computed orders of the potential. This is in contrast with the Δ-less theory, where at NLO-$\not\Delta$ the deuteron became unbound (as discussed extensively in Ref. [30]).

TABLE IV. Deuteron properties for the OPE and TPE potentials. The computation is made by fixing γ and η to their experimental values. The errors quoted in both TPE computations reflect the uncertainty in the nonpotential parameters γ, η, and α_0 only. For the OPE (LO) we take $g_{\pi NN} = 13.1(1)$. For the LEC's in the TPE calculation, by set IV we refer to the determination of Ref. [24] (see main text). For the Δ case we use Fits 1 and 2 of Ref. [52]. Fit 1 involves the SU(4) quark-model relation $h_A = 3g_A/(2\sqrt{2}) = 1.34$ for $g_A = 1.26$. Fit 2 takes $h_A = 1.05$. The experimental values are taken from the following references: η from Ref. [63], A_S from Ref. [64], r_m from Ref. [65], and Q_d from Ref. [66] (see also Ref. [67] for a brief review).

Set	γ (fm^{-1})	η	A_S (fm$^{-1/2}$)	r_m (fm)	Q_d (fm^2)	P_D (%)	$\langle r^{-1}\rangle$	$\langle r^{-2}\rangle$
LO	Input	0.02633	0.8681(1)	1.9351(5)	0.2762(1)	7.31(1)	0.486(1)	0.434(3)
NLO-$\not\Delta$	Unbound	–	–	–	–	–	–	–
NLO-Δ ($h_A = 1.34$)	Input	Input	0.884(3)	1.963(7)	0.274(9)	5.9(4)	0.446(10)	0.29(2)
NLO-Δ ($h_A = 1.05$)	Input	Input	0.84(4)	1.86(8)	0.24(3)	12(5)	0.62(15)	0.8(4)
N2LO-$\not\Delta$ (Set IV)	Input	Input	0.884(4)	1.967(6)	0.276(3)	8(1)	0.447(5)	0.284(8)
N2LO-$\not\Delta$ (πN)	Input	Input	0.896(2)	1.990(3)	0.282(5)	6.1(8)	0.4287(13)	0.253(2)
N2LO-Δ(Fit 1)	Input	Input	0.892(2)	1.980(4)	0.279(5)	5.9(9)	0.4336(15)	0.262(3)
N2LO-Δ(Fit 2)	Input	Input	0.890(2)	1.975(3)	0.278(5)	5.8(9)	0.4470(15)	0.268(2)
NijmII	0.231605	0.02521	0.8845	1.9675	0.2707	5.635	0.4502	0.2868
Reid93	0.231605	0.02514	0.8845	1.9686	0.2703	5.699	0.4515	0.2924
Exp.	0.231605	0.0256(4)	0.8838(4)	1.971(5)	0.2860(15)	–	–	–

Here, we also compute the matter radius, which reads,

$$r_m^2 = \frac{\langle r^2\rangle}{4} = \frac{1}{4}\int_0^\infty r^2[u(r)^2 + w(r)^2]dr, \tag{48}$$

the quadrupole moment (without meson exchange currents)

$$Q_d = \frac{1}{20}\int_0^\infty r^2 w(r)[2\sqrt{2}u(r) - w(r)]dr, \tag{49}$$

the D-state probability

$$P_D = \int_0^\infty w(r)^2 dr, \tag{50}$$

and the inverse moments of the radius

$$\langle r^{-n}\rangle = \int_0^\infty r^{-n}(u(r)^2 + w(r)^2)dr, \tag{51}$$

which, as is well known, appear in the multiple scattering expansion of the π-deuteron scattering length. Some results for the inverse moments in Δ-less effective field theory can be found in Refs. [59,68]. In Table IV we show our results in a variety of situations. In general, the results for NLO-Δ and N2LO-Δ are in agreement with the experimental value of the deuteron observables, with the exception of the quadrupole moment, which presents a discrepancy of 0.01 fm^2. The reason for it lies in meson exchange current contributions to the quadrupole moment, which were estimated for ChPT in Ref. [69] and are of the order of the difference of our results with respect to the experimental value. When comparing the Δ-full computations with the Δ-less ones, one can notice, first, that a renormalized result exists for NLO-Δ, unlike the NLO-$\not\Delta$ case (as was explained in more detail in Ref. [30]). This supports the better convergence properties of effective theory when including the Δ degree of freedom. It can also be noticed that the D-wave probability P_D, although not an observable, it is better described in N2LO-Δ than in N2LO-$\not\Delta$, when compared with the results coming from the phenomenological

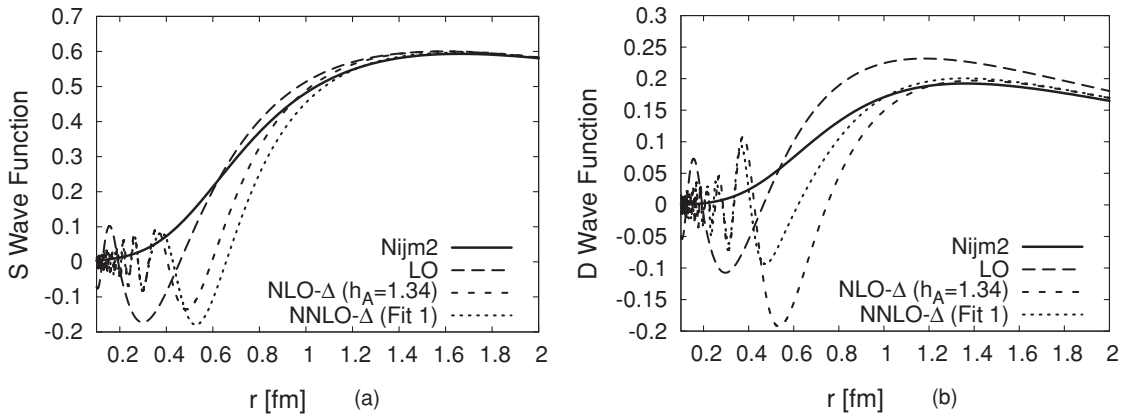

FIG. 2. Deuteron wave functions, u (left panel) and w (right panel), as a function of the distance (in fm) for the LO, NLO-Δ, and N2LO-Δ potentials, compared to the Nijmegen II wave functions [6]. The asymptotic normalization $u(r) \to e^{-\gamma r}$ has been adopted and the asymptotic D/S ratio is taken $\eta = 0.0256(4)$. The oscillations of the wave functions are related to the presence of deeply bound states but do not have any appreciable effect on deuteron observables as they cannot be resolved in effective field theory.

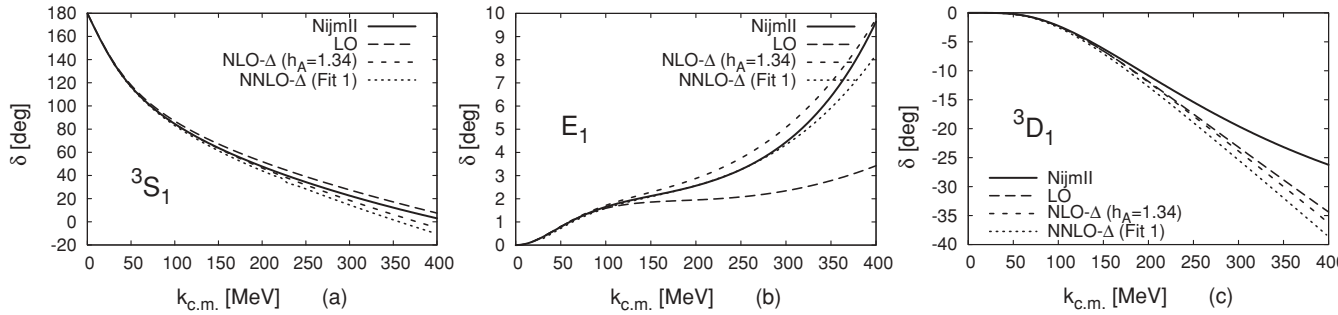

FIG. 3. np spin triplet (eigen-)phase shifts for total angular momentum $j = 1$ as a function of the center-of-mass momentum compared to the Nijmegen II potential phase shifts [6].

potentials [67]. The consequence is that the magnetic moment of the deuteron would be better described in the Δ-full theory than in the Δ-less theory, although no actual computation has been made on that respect in the present article. The reason for that is that in a nonrelativistic framework, the deuteron magnetic moment depends solely on P_D [70]. Before comparing the results for other observables, one important comment must be made: one should only directly compare the N2LO-Δ results with the N2LO-$\not\Delta$ (πN) ones. Comparison with N2LO-$\not\Delta$ set IV should be done with care, as for this case the LECs are fitted to reproduce NN data [24]. This is why they look slightly better than the other results of Table IV. Therefore, the comparison of N2LO-Δ with N2LO-$\not\Delta$ (πN) results implies in particular that the inclusion of Δ enhances the compatibility between πN and NN scattering, as one would expect within the EFT philosophy.

C. Phase shifts

Finally, in the case of positive energy we consider Eq. (36) with

$$E_{\text{c.m.}} = \frac{k^2}{M} \tag{52}$$

where k is the corresponding center-of-mass momentum. We solve Eq. (36) for the two linear independent scattering states, which are usually labeled as the α and β states. They are defined by the asymptotic normalization

$$\begin{aligned} u_{k,\alpha}(r) &\to \cos\epsilon[\hat{j}_0(kr)\cot\delta_1 - \hat{y}_0(kr)], \\ w_{k,\alpha}(r) &\to \sin\epsilon[\hat{j}_2(kr)\cot\delta_1 - \hat{y}_2(kr)], \end{aligned} \tag{53}$$

$$\begin{aligned} u_{k,\beta}(r) &\to -\sin\epsilon[\hat{j}_0(kr)\cot\delta_2 - \hat{y}_0(kr)], \\ w_{k,\beta}(r) &\to \cos\epsilon[\hat{j}_2(kr)\cot\delta_2 - \hat{y}_2(kr)], \end{aligned} \tag{54}$$

where $\hat{j}_l(x) = x j_l(x)$ and $\hat{y}_l(x) = x y_l(x)$ are the reduced spherical Bessel functions and δ_1 and δ_2 are the eigenphases in the $^3S_1$ and $^3D_1$ channels; ε is the mixing angle E_1. The orthogonality constraints between the deuteron and scattering states generate the following boundary conditions

$$\begin{aligned} u_\gamma u'_{k,\alpha} - u'_\gamma u_{k,\alpha} + w_\gamma w'_{k,\alpha} - w'_\gamma u_{k,\alpha}|_{r=r_c} &= 0, \\ u_\gamma u'_{k,\beta} - u'_\gamma u_{k,\beta} + w_\gamma w'_{k,\beta} - w'_\gamma u_{k,\beta}|_{r=r_c} &= 0. \end{aligned} \tag{55}$$

The use of the superposition principle for the α- and β-scattering states, plus the deuteron wave functions, deduction of the corresponding $^3S_1$-$^3D_1$ eigenphase shifts. The results are depicted in Fig. 3 at LO, NLO-Δ, and N2LO-Δ compared to the Nijmegen II potential results [6]. We observe a clear improvement in the threshold region and quite remarkably for the E_1 mixing phase. However, there is no improvement in the $^3D_1$ phase shift.

V. COMPARISON WITH THE Δ-LESS THEORY

In our previous work [30], the renormalization of Δ-less theory was analyzed. As discussed above, it was found that at NLO-$\not\Delta$ there was no deuteron bound state if the cutoff was removed. The reason was due to the short-distance $\sim g_A^4/(f_\pi^4 r^5)$ repulsive singular character of the potential in the $^3S_1$-$^3D_1$ channel. However, at N2LO-$\not\Delta$ three counterterms were needed due to the short-distance attractive singular character of the potential. In fact the agreement with more sophisticated calculations [24] was remarkable. More recently, the quality of these chiral wave functions has been tested in electron-deuteron scattering [43] using LO currents, with an amazingly good agreement up to momentum transfer of $q = 1$ GeV. It is interesting to compare the results of the Δ-less theory [30] with the ones found here after inclusion of the Δ in the potential. The first aspect to note is that the NLO-Δ potential has an attractive $\sim g_A^4/(\Delta f_\pi^4 r^6)$ short-distance singularity, a feature kept at the N2LO-Δ; however, with different scales.

In Fig. 4 the np $^1S_0$ singlet phase shifts are depicted as a function of the center-of-mass momentum for the N2LO-Δ and N2LO-$\not\Delta$ compared to the Nijmegen II potential phase shifts [6]. As we see, with only one counterterm, i.e., fixing the scattering length α_0, the result is slightly worsened when the Δ is included. This is consistent with the change in the effective range reported in Table III. Of course, if r_0 is fixed as an additional renormalization condition, there is an improvement in the low-energy region but the difference between including or not Δ degrees of freedom is hardly visible.

The situation for the deuteron wave functions is slightly different. As we see in Fig. 5, the present N2LO-Δ deuteron wave functions resemble slightly better the Nijmegen II ones

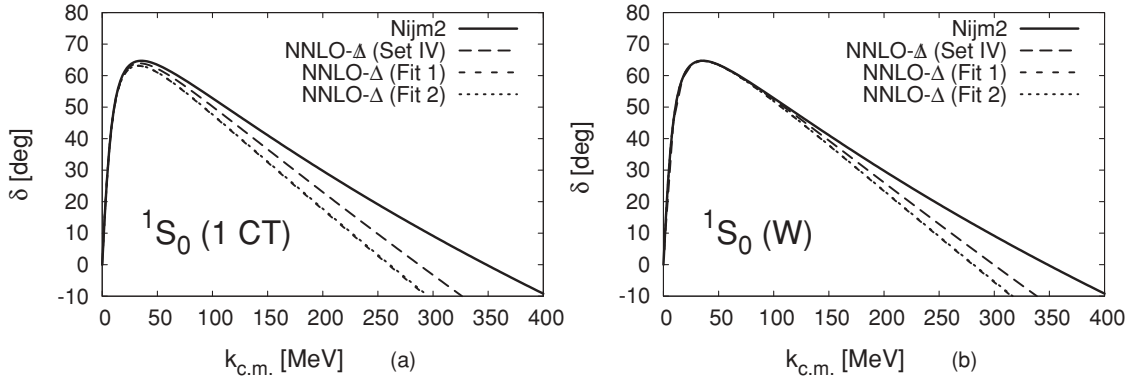

FIG. 4. The np spin singlet phase shifts as a function of the center-of-mass momentum for the N2LO-⧋ and N2LO-Δ potentials, with one counterterm (left panel) and two counterterms (right panel) compared to the Nijmegen II potential results [6].

[5,6]. In particular, the D-wave becomes smaller when one goes from our previous TPE ones [30].

Finally, in Fig. 6 we show the np eigenphase shifts in the $^3S_1$-$^3D_1$ channel as a function of the center-of-mass momentum for the N2LO-Δ and N2LO-⧋ compared to the Nijmegen II potential results [6]. The noticeable improvement in the E_1 phase is in agreement with the smaller D-wave deuteron wave function.

VI. SCHEME DEPENDENCE AND CUTOFFS

A. The relevant scales

As we see our scheme including the Δ does not reproduce the $^1S_0$ phase shift for momenta larger than the pion mass even if the effective range is adjusted to its experimental value. This trend has also been observed in other renormalized calculations including TPE effects and $1/M$ corrections in a heavy baryon formalism [30], using a relativistic potential [71] or including N3LO two-pion exchange contributions [42].[9] In the next paragraphs we discuss the main candidates for such a disagreement.

It is interesting at this point to ask which are the relevant scales that build the full strength of the phase shifts. As already found in Refs. [29–31,42,71] this is about 0.4–0.5 fm for Δ-less calculations. For illustration purposes, the short-distance cutoff dependence is shown in Fig. 7 for the effective range in the case of renormalization with one counterterm in the heavy baryon Δ-less theory to LO, NLO-⧋, and N2LO-⧋ where also the Nijmegen II potential [6] is considered. As we see, and regardless on the full renormalized effective range value, the Nijmegen II saturating scale is in between NLO-⧋ and N2LO-⧋, a not unreasonable result. Likewise, the N2LO-Δ effective range displays a similar approach to the renormalized result.

These scales are comparable to the nucleon size but also to the range where 3π exchange starts contributing because it behaves as $e^{-3m_\pi r}$ at long distances. According to the results of Kaiser [72–74] (and in the absence of Δ) the potential is attractive and, using dimensional estimates for the 3π-exchange potential, it behaves as $g_A^6/(f_\pi^6 r^7)$ at short distances, indicating a stronger singularity and therefore a stronger short distance $u(r) \sim r^{\frac{7}{4}}$ suppression as well. Thus,

[9] For an N3LO NN-scattering calculation which explicitly includes 3π exchange see Ref. [28].

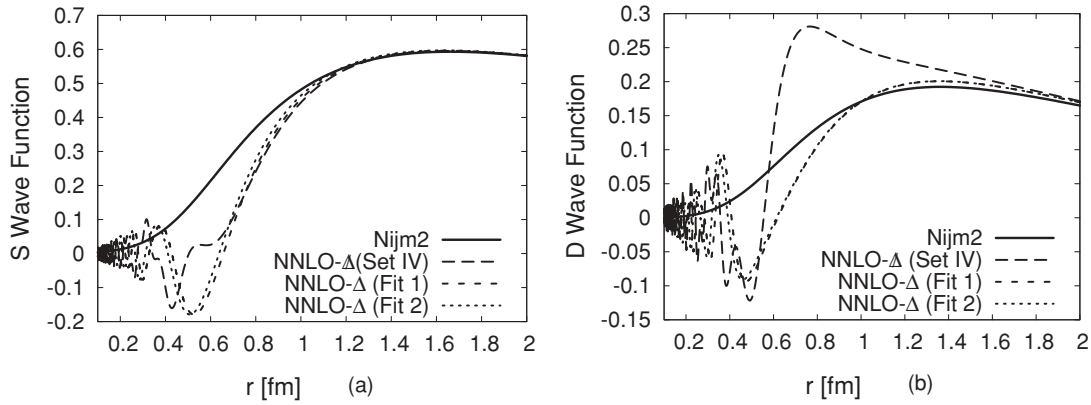

FIG. 5. Deuteron wave functions, u (left panel) and w (right panel), as a function of the radius (in fm) for the N2LO-⧋ potential and the NLO and N2LO-Δ potentials, compared to the Nijmegen II wave functions [6]. The asymptotic normalization $u \to e^{-\gamma r}$ has been adopted and the value $\eta = 0.0256(4)$ is taken for the asymptotic D/S ratio.

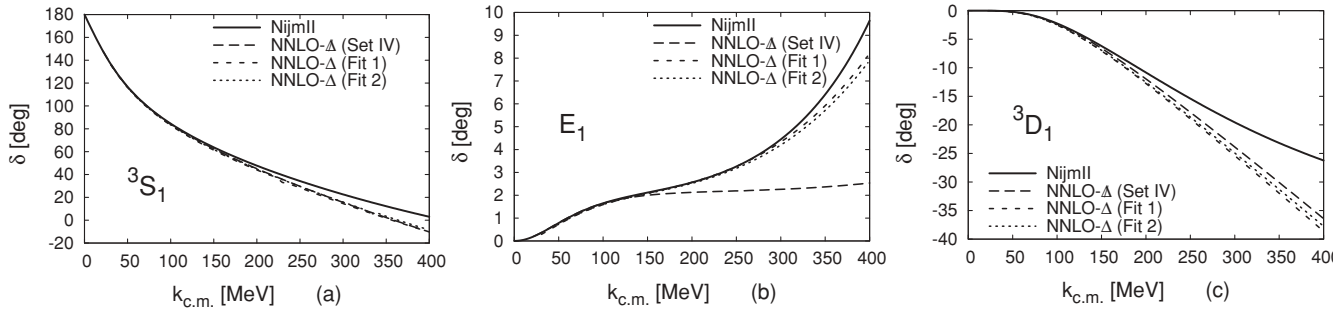

FIG. 6. The np spin triplet (eigen-)phase shifts for the total angular momentum $j = 1$ as a function of the center-of-mass momentum for the N2LO-Δ and N2LO-$\not\Delta$ potentials compared to the Nijmegen II potential results [5,6].

we expect that including these effects would only slightly worsen the results by reducing the phase shift. In addition, according to the N3LO NN computation of Ref. [28], the effect of 3π exchanges is negligible.

Another interesting observation is that by taking larger coordinate space cutoffs the phase shift is not improved, as in our regularization procedure it converges from below, so in this case the best possible cutoff is $r_c \to 0$.[10] In this context, one can identify two kinds of finite cutoff sources of errors: the first one is related with the explicit form of the regulator employed in the computations and the second one with the actual size of the finite cutoff. This second source of errors is the only one that is usually assessed in most effective field theory works, while the role played by the regulator is commonly ignored, probably resulting in an underestimation of the errors. Although in our present renormalization scheme the most sensible thing to do in the $^1S_0$ singlet channel is to completely remove the cutoff, this may be not be the case in other regularization schemes. Although this could be in fact considered as a good motivation for keeping a finite cutoff or introducing form factors, we think that this kind of procedure is difficult to justify from the EFT viewpoint.

The influence of relativistic effects on the results is less obvious, because they generate either energy dependence or nonlocalities, but experience in renormalizing relativistic potentials indicates that they are not crucial, at least in the $^1S_0$ channel [71], and are saturated by scales larger than the nucleon Compton wavelength, i.e., well above a possible influence from the $N\bar{N}$ channel.

Thus, we see that in all these calculations including TPE effects the saturating scales are of the order of 0.5 fm, regardless on detailed issues, in particular including or not the Δ. This is comparable to other scales, $2/m_\rho \sim 0.51$ fm, which may equally represent vector-meson exchange or nucleon size effects. Therefore the discrepancy between renormalized phase shifts and phenomenological ones should be considered a real one, in the sense that finite size effects may be important physically. Moreover, it should be kept in mind that once the short-distance cutoff becomes smaller than the nucleon size, the effect of the counterterms is not enough to reproduce intermediate energy phase shifts, meaning that they cannot mimic the finite nucleon size or other short-distance physical effects that may be responsible for the observed discrepancy.

[10]Improving or not the phase shifts by using a finite cutoff while keeping the same renormalization conditions is, in fact, a regularization scheme-dependent feature and hence a further good reason to remove the cutoff. This choice, however, does not resolve the representation dependence of the potential on the choice of the pion field. Therefore, the cutoff less solution will obviously depend on the previous choice.

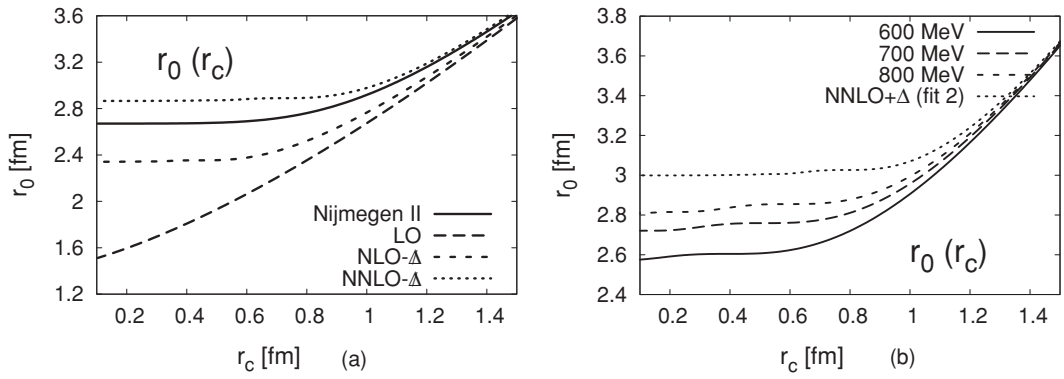

FIG. 7. $^1S_0$ effective range (in fm) $r_0(r_c) = 2\,[\int_0^\infty (1 - r/\alpha_0)^2\,dr - \int_{r_c}^\infty u_0^2\,dr]$, with $\alpha_0 = -23.74$ fm as a function of the short-distance cutoff r_c (in fm). We compare the (heavy baryon) Δ-less theory at LO, NLO, and N2LO and the Nijmegen II potential [6] (left panel) with the spectral-regularized N2LO-Δ potential for different values of the spectral cutoff $\tilde{\Lambda}$ (right panel).

B. Remarks on spectral regularization

The calculation of the NN potentials can advantageously be carried out by using the method of dispersion relations [13,14,52]. This has motivated the use of the so-called spectral regularization [26–28,52] in NN calculations where finite momentum space cutoffs have been implemented. Remarkably, a good fit to the $^1S_0$ phase was achieved. This is in contrast to the N3LO computation carried out in Ref. [42] with one counterterm, where a systematic underestimation of the data was found. In our view, the relevant issue is to disentangle the cutoff artifacts from clearly attributable physical effects. In this section we analyze the issue of cutting off the potential.

The two-pion exchange potential satisfies a dispersion relation based on the $N\bar{N} \to 2\pi$ amplitude. One has the representations

$$V_C(r,\tilde{\Lambda}) = \frac{1}{2\pi^2 r}\int_{2m}^{\tilde{\Lambda}} d\mu\,\mu\rho_C(\mu)e^{-\mu r},$$

$$V_S(r,\tilde{\Lambda}) = -\frac{1}{6\pi^2 r}\int_{2m}^{\tilde{\Lambda}} d\mu\,\mu(\mu^2\rho_T(\mu) - 3\rho_S(\mu))e^{-\mu r},$$

$$V_T(r,\tilde{\Lambda}) = -\frac{1}{6\pi^2 r^3}\int_{2m}^{\tilde{\Lambda}} d\mu\,\mu^3(3+3\mu r+\mu^2 r^2)\rho_T(\mu)e^{-\mu r}, \tag{56}$$

with $\rho_i(\mu) = \mathrm{Im}V_i(i\mu)$ and similar relations for the W_i potentials. It is straightforward to see that for small $\tilde{\Lambda}$ and $r \ll \tilde{\Lambda}^{-1}$, the potentials behave as

$$V_C(r,\tilde{\Lambda}) \to \frac{1}{2\pi^2 r}\int_{2m}^{\tilde{\Lambda}} d\mu\,\mu\rho_C(\mu),$$

$$V_S(r,\tilde{\Lambda}) \to -\frac{1}{6\pi^2 r}\int_{2m}^{\tilde{\Lambda}} d\mu\,\mu[\mu^2\rho_T(\mu) - 3\rho_S(\mu)], \tag{57}$$

$$V_T(r,\tilde{\Lambda}) \to -\frac{1}{6\pi^2 r^3}\int_{2m}^{\tilde{\Lambda}} d\mu\,\mu^3\,3\rho_T(\mu).$$

Thus, although V_C, W_C, V_S, and W_S become regular, the tensor contributions V_T and W_T remain singular, despite higher-energy states being cut off. That means that regularization of the scattering problem in triplet channels is mandatory to obtain well-defined results.

Note that this short-distance behavior is quite different from the one obtained for $r > 0$ when $\tilde{\Lambda} \to \infty$ (see Appendix). In Fig. 8 the ratio $V(r,\tilde{\Lambda})/V(r)$ of $^1S_0$ potentials as they enter in the phase-shift calculation with and without spectral regularization is depicted. We note that there is a sizable distortion at 2–3 fm's with $\tilde{\Lambda} = 700$ MeV, decreasing the strength of the interaction and hence providing effectively a repulsion in the singlet potential. The effects of the spectral regularization on the potential for N2LO-Δ both with one counterterm as well as with two counterterms can be seen in Figs. 9(a) and 9(b) respectively. As we see, it is possible to describe the data successfully for suitable values of the spectral cutoff $\tilde{\Lambda} \sim 700$ MeV, in agreement with the findings of Ref. [52]. It is noteworthy that this happens *regardless* on the usage

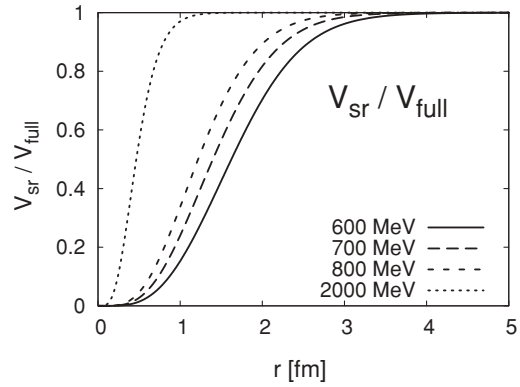

FIG. 8. $V(r,\Lambda)/V(r)$-ratio of $^1S_0$ potentials as a function of the distance r (in fm) for the spectral-regularized N2LO-Δ potential with different values of the spectral cutoff $\tilde{\Lambda}$ as a function of the short distance cutoff r_c (in fm).

of one or two counterterms, reinforcing the conclusion that the agreement is mainly due to the distortion in the potential. In regard to the behavior with respect to spectral regularization, the trends presented for the Δ-full theory are also reproduced in the Δ-less scheme. We note that an accurate description of the data was achieved in Ref. [28] at N3LO-$\not\Delta$ with a spectral regularized potential with finite momentum space cutoffs and 4 counterterms in the $^1S_0$ channel (the full N3LO computation has 24 counterterms). On the other hand, the data were not described for large values of p in the N3LO-$\not\Delta$ and (spectrally) unregularized renormalized calculation of Ref. [42].

As before, it is interesting to analyze the relevant scales building up the effective range in the case of renormalization with one counterterm. In Fig. 7, we show the effective range r_0 as a function of the short-distance cutoff r_c for several values of the spectral cutoff $\tilde{\Lambda}$. Clearly, the stability region in r_c is shifted toward lower values as the spectral cutoff is decreased. This is consistent with the large distortion of the potential at intermediate scales.

We have also analyzed the impact of the spectral regularization on the already successful description of the deuteron presented in previous articles and the present one. The results do not change noticeably after (spectrally) regularizing the potential: they lie between the results obtained with the OPE potential and with NLO- and N2LO-Δ. This is compatible with the weakening of these contributions to the chiral potential. Although the final results are rather simple to summarize, some remarks should be added on the renormalization procedure for the deuteron channel when spectral regularization is applied. The modified NLO- and N2LO-Δ chiral potentials have now an attractive and repulsive eigenchannel, instead two attractive ones, which lead us to the following alternative: either we remove the cutoff, in which case we can only fix the binding energy and obtain the D/S ratio η as a prediction, or we keep a finite cutoff and then fix both the binding energy and η. Provided that the finite cutoff is sensible, about $r_c \sim 0.5$ fm (i.e., the saturation scale) for a spectral cutoff $\tilde{\Lambda} \sim 600$–800 MeV, both procedures give equivalent results. The

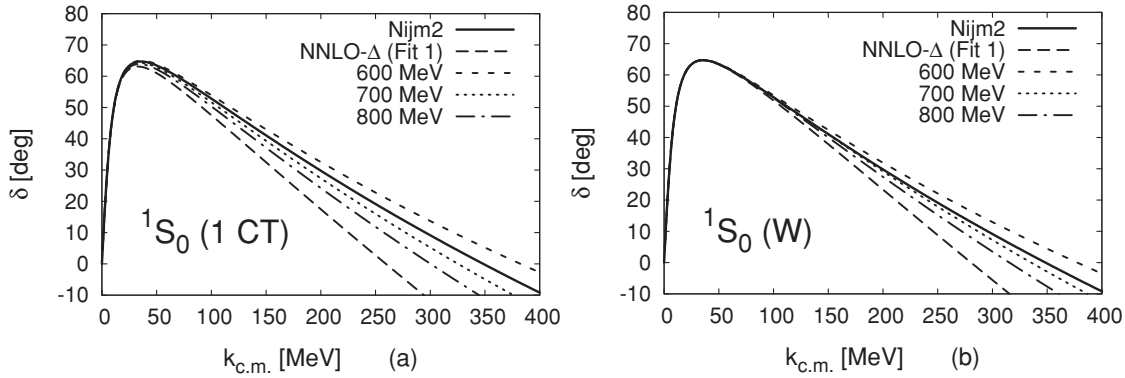

FIG. 9. np $^1S_0$ renormalized phase shifts for the spectral-regularized N2LO-Δ potential for different values of the spectral cutoff $\tilde{\Lambda}$ as a function of the center-of-mass momentum (in MeV) compared to the Nijmegen II potential results [6] with one counterterm (left panel) and with two counterterms (right panel), corresponding this last choice to the standard Weinberg counting.

previous discussion on the effects of spectral cutoff agree with the remarks presented in Ref. [43] regarding the effects of this regularization of the potential for the deuteron form factors. For completeness we show the results in Table V.

In summary, reducing the strength of the potential at short distances by means of the spectral regularization is phenomenologically preferred in the singlet channel and innocuous in the triplet channel but distorts largely the chiral

TABLE V. Deuteron properties for the OPE and TPE potentials with spectral regularization. The computation is made by fixing γ and η to their experimental values or by fixing γ and predicting η depending on the singularity structure of the potential and the coordinate space cutoff. For each case we present three computations: (i) the complete computation, i.e., the results obtained when the cutoff is completely removed and there is no spectral cutoff; (ii) the spectrally regularized computation with $r_c = 0.1$ fm; and (iii) the spectrally regularized computation with $r_c = 0.5$ fm. The errors quoted in the (spectrally) unregularized TPE computations and in the spectrally regularized potential with a finite cutoff $r_c = 0.5$ fm reflect the uncertainty in the nonpotential parameters γ and η. In the spectrally regularized potentials, the errors represent the cutoff dependence of the results for r_c ranging from 0.1 to 0.2 fm. For the OPE (LO) we take $g_{\pi NN} = 13.1(1)$. We take set IV [24] for the LEC's in the TPE calculation. For the Δ case we use Fits 1 and 2 of Ref. [52]. Fit 1 involves the SU(4) quark-model relation $h_A = 3g_A/(2\sqrt{2}) = 1.34$ for $g_A = 1.26$. Fit 2 takes $h_A = 1.05$.

Set	γ (fm^{-1})	η	A_S (fm$^{-1/2}$)	r_m (fm)	Q_d (fm^2)	P_D (%)	$\langle r^{-1}\rangle$	$\langle r^{-2}\rangle$
LO	Input	0.02633	0.8681(1)	1.9351(5)	0.2762(1)	7.31(1)	0.486(1)	0.434(3)
NLO-$\not\Delta$	Unbound	–	–	–	–	–	–	–
$\tilde{\Lambda} = 700$ MeV	Input	0.02669	0.851(7)	1.894(15)	0.270(4)	8.9(1.0)	0.6(2)	1.8(1.5)
$r_c = 0.5$ fm	Input	Input	0.83(2)	1.86(6)	0.24(2)	8(3)	0.56(7)	0.51(15)
NLO-Δ ($h_A = 1.34$)	Input	Input	0.884(3)	1.963(7)	0.274(9)	5.9(4)	0.446(10)	0.29(2)
$\tilde{\Lambda} = 700$ MeV	Input	0.02637	0.8720(10)	1.938(2)	0.2781(6)	7.31(12)	0.48(2)	0.5(2)
$r_c = 0.5$ fm	Input	Input	0.867(13)	1.93(3)	0.263(14)	6.6(1.2)	0.48(4)	0.35(8)
NLO-Δ ($h_A = 1.05$)	Input	Input	0.84(4)	1.86(8)	0.24(3)	12(5)	0.62(15)	0.8(4)
$\tilde{\Lambda} = 700$ MeV	Input	0.02651	0.864(2)	1.922(5)	0.2755(14)	7.8(3)	0.52(5)	0.7(4)
$r_c = 0.5$ fm	Input	Input	0.854(17)	1.90(4)	0.26(2)	7(2)	0.51(5)	0.41(11)
N2LO-$\not\Delta$ (Set IV)	Input	Input	0.884(4)	1.967(6)	0.276(3)	8(1)	0.447(5)	0.284(8)
$\tilde{\Lambda} = 700$ MeV	Input	0.02504	0.877(2)	1.946(5)	0.264(2)	5.6(7)	0.48(2)	0.42(6)
$r_c = 0.5$ fm	Input	Input	0.875(8)	1.942(15)	0.270(2)	8(2)	0.46(2)	0.27(6)
N2LO-$\not\Delta$ (πN)	Input	Input	0.896(2)	1.990(3)	0.282(5)	6.1(8)	0.4287(13)	0.253(2)
$\tilde{\Lambda} = 700$ MeV	Input	0.02590	0.8801(2)	1.9540(5)	0.27659(14)	6.580(6)	0.463(4)	0.35(3)
$r_c = 0.5$ fm	Input	Input	0.883(4)	1.956(6)	0.274(9)	5.9(8)	0.447(13)	0.28(2)
N2LO-Δ (Fit 1)	Input	Input	0.892(2)	1.980(4)	0.279(5)	5.9(9)	0.4336(15)	0.262(3)
$\tilde{\Lambda} = 700$ MeV	Input	0.02603	0.8783(3)	1.9507(6)	0.2774(2)	6.77(3)	0.465(4)	0.36(4)
$r_c = 0.5$ fm	Input	Input	0.880(6)	1.954(14)	0.272(10)	5.9(6)	0.45(2)	0.29(4)
N2LO-Δ (Fit 2)	Input	Input	0.890(2)	1.975(3)	0.278(5)	5.8(9)	0.4470(15)	0.268(2)
$\tilde{\Lambda} = 700$ MeV	Input	0.02606	0.8769(4)	1.9479(7)	0.2770(2)	6.83(3)	0.467(5)	0.37(4)
$r_c = 0.5$ fm	Input	Input	0.878(6)	1.950(15)	0.271(10)	5.9(6)	0.46(2)	0.30(4)
Nijm II	0.231605	0.02521	0.8845	1.9675	5.635	0.2707	0.4502	0.2868
Reid 93	0.231605	0.02514	0.8845	1.9686	0.2703	5.699	0.4515	0.2924
Exp.	0.231605	0.0256(4)	0.8838(4)	1.971(5)	0.2860(15)	–	–	–

potential in a region much larger than the nucleon size. Moreover, we find that within our scheme the agreement with the data is achieved *regardless* of the additional counterterms invoked by Weinberg's counting, being in fact superfluous after renormalization. This said, although the spectral regularization improves over the standard finite cutoff approaches and seems phenomenologically favored, the inclusion of finite-size effects in a model-independent manner would certainly be very useful.

VII. CONCLUSIONS

Since the early 1990s there has been a growing interest in pursuing an EFT description of NN scattering below the pion production threshold where the spontaneous breakdown of chiral symmetry in QCD is manifestly exploited. One of the reasons that has greatly hindered the EFT developments within the NN context has been the lack of a credible power counting for the potential that at the same time complies to short-distance insensitivity. Given the tight constraints under which this might actually happen, it has not been obvious which particular form of the chiral expansion indeed embodies these desirable properties. In the present work we have shown how the inclusion of Δ degrees of freedom in the potential not only complies to a phenomenologically well-founded motivation but also provides the requested short-distance insensitivity of the central phases and the deuteron properties after the necessary renormalization is carried out. This improves the previous situation without explicit Δ degrees of freedom: while at LO-$\not\Delta$ and N2LO-$\not\Delta$ the existence of a deuteron was compatible with renormalizability; at NLO-$\not\Delta$ that was not the case. This has raised reasonable doubts on the suitability and usefulness of nonperturbative renormalization *per se* to chiral potentials. A very rewarding aspect of the present investigation is the existence of a deuteron bound state at LO, NLO-Δ, and N2LO-Δ. Of course, a proof of consistency to all orders, including relativistic, spin-orbit, three-pion exchange corrections, etc., remains to be done. This is so because, although the power law behavior of the chiral potential at short distances can be trivially fixed by dimensional arguments and power counting, the determination of the attractive-repulsive character of the potential can so far only be fixed by actual calculations. The found deuteron properties seem to obey a converging pattern and in the E_1 phase a clear improvement is observed at N2LO-Δ. Moreover, our N2LO-Δ results resemble much those of N2LO-$\not\Delta$ after renormalization for reasonable parameter values describing the πN reaction close to threshold. This suggests that despite the previous inconsistency in NLO-$\not\Delta$, the N2LO-$\not\Delta$ deuteron wave functions can be used for practical purposes, despite the theoretically unpleasant and disturbing "jumping" of the NLO-$\not\Delta$ calculation. In addition, it should be noted that within these approximations the πN threshold properties can be fitted, with the sole exception of $b_{0,+}^-$, and thus the overall consistency between the πN and NN sectors is almost satisfied. Therefore, the inclusion of the Δ resonance complies with the original EFT motivation of describing *simultaneously* πN and NN scattering at low energies.

We have also found that at the level of approximations involved in the present and previous renormalized calculations, the $^1S_0$ phase shift is not entirely reproduced for center-of-mass momenta larger than the pion mass if we insist on a reasonable πN physics. Several effects might be responsible for this persistent discrepancy. We have discussed those on the light of the relevant scales, $r \geqslant r_c = 0.5$ fm, which practically provide the total contribution to observables. We have further discussed parametrizations of the NN force based on a spectral regularization of the NN potential with a cutoff of $\tilde{\Lambda} = 700$ MeV. We have shown that agreement to data is achieved mainly due to a large distortion of the potential at 2–3 fm and regardless on additional inclusion of counterterms. These length scales are much larger than the expected finite nucleon size or vector meson exchange effects, casting doubts on the usefulness of spectral regularization and suggesting the need for a more controllable and better founded description of the missing short distance physics in the $^1S_0$ channel.

In the present article we have restricted to central phases and the deuteron, but the calculation of higher partial waves is also of interest, as well as the inclusion of Coulomb effects in pp scattering. In all cases, the negative definite character of the potential at short distances guarantees the existence of convergent results. Finally, the present results can have some impact on calculations, including deuteron properties such as deuteron form factors, pion-deuteron scattering, and further low-energy matrix elements of electroweak deuteron reactions where short-distance insensitivity and chiral symmetry are both expected to play a significant role.

ACKNOWLEDGMENTS

We thank Andreas Nogga, Evgeny Epelbaum, Ulf-G. Meißner, and Johann Haidenbauer for discussions and a critical and careful reading of the manuscript. M.P.V. is supported by the Helmholtz Association fund provided to the young investigator group "Few-Nucleon Systems in Chiral Effective Field Theory" (Grant VH-NG-222) and to the virtual institute "Spin and Strong QCD" (VH-VI-231). The work of E.R.A. is supported in part by funds provided by the Spanish DGI and FEDER funds with Grant No. FIS2008-01143/FIS, Junta de Andalucía Grants No. FQM225-05, and EU Integrated Infrastructure Initiative Hadron Physics Project Contract No. RII3-CT-2004-506078.

APPENDIX: SHORT-DISTANCE EXPANSION OF THE POTENTIALS

Using the spectral representation the short-distance expansion of the potentials can be done by expanding spectral functions for $\mu \gg m$, with μr fixed. This way one obtains

$$V_C(r) = \frac{C_6^{V,C}}{r^6} + \cdots$$

$$W_C(r) = \frac{C_6^{W,C}}{r^6} + \cdots$$

$$V_S(r) = \frac{C_6^{V,S}}{r^6} + \cdots$$
$$W_S(r) = \frac{C_6^{W,S}}{r^6} + \cdots$$
$$V_T(r) = \frac{C_6^{V,T}}{r^6} + \cdots$$
$$W_T(r) = \frac{C_6^{W,T}}{r^6} + \cdots \tag{A1}$$

where the van der Waals coefficients at NLO-Δ are given by

$$C_{6,V,C}^{\text{NLO-}\Delta} = -\frac{\left(9g_A^2 + 4h_A^2\right)h_A^2}{36 f_\pi^4 \pi^2 \Delta} \tag{A2}$$

$$C_{6,W,C}^{\text{NLO-}\Delta} = -\frac{\left(9g_A^2 - 2h_A^2\right)h_A^2}{108 f_\pi^4 \pi^2 \Delta} \tag{A3}$$

$$C_{6,V,S}^{\text{NLO-}\Delta} = \frac{\left(9g_A^2 - 2h_A^2\right)h_A^2}{216 f_\pi^4 \pi^2 \Delta} \tag{A4}$$

$$C_{6,W,S}^{\text{NLO-}\Delta} = \frac{\left(9g_A^2 + h_A^2\right)h_A^2}{648 f_\pi^4 \pi^2 \Delta} \tag{A5}$$

$$C_{6,V,T}^{\text{NLO-}\Delta} = -\frac{\left(9g_A^2 - 2h_A^2\right)h_A^2}{216 f_\pi^4 \pi^2 \Delta} \tag{A6}$$

$$C_{6,W,T}^{\text{NLO-}\Delta} = -\frac{\left(9g_A^2 + h_A^2\right)h_A^2}{648 f_\pi^4 \pi^2 \Delta} \tag{A7}$$

and at N2LO-Δ by

$$C_{6,V,C}^{\text{N2LO-}\Delta} = \frac{4\tilde{b}\, h_A^3}{9 f_\pi^4 \pi^2} + \frac{c_3 h_A^2}{f_\pi^4 \pi^2} + \frac{9 c_3 g_A^2}{16 f_\pi^4 \pi^2} \tag{A8}$$

$$C_{6,W,C}^{\text{N2LO-}\Delta} = \frac{2\tilde{b}\, h_A^3}{27 f_\pi^4 \pi^2} - \frac{\tilde{b}\, g_A^2 h_A}{6 f_\pi^4 \pi^2} \tag{A9}$$

$$C_{6,V,S}^{\text{N2LO-}\Delta} = \frac{\tilde{b}\, g_A^2 h_A}{12 f_\pi^4 \pi^2} - \frac{\tilde{b}\, h_A^3}{27 f_\pi^4 \pi^2} \tag{A10}$$

$$C_{6,W,S}^{\text{N2LO-}\Delta} = -\frac{\tilde{b}\, h_A^3}{162 f_\pi^4 \pi^2} + \frac{c_4 h_A^2}{36 f_\pi^4 \pi^2} + \frac{c_4 g_A^2}{16 f_\pi^4 \pi^2} \tag{A11}$$

$$C_{6,V,T}^{\text{N2LO-}\Delta} = \frac{\tilde{b}\, h_A^3}{27 f_\pi^4 \pi^2} - \frac{\tilde{b}\, g_A^2 h_A}{12 f_\pi^4 \pi^2} \tag{A12}$$

$$C_{6,W,T}^{\text{N2LO-}\Delta} = \frac{\tilde{b}\, h_A^3}{162 f_\pi^4 \pi^2} - \frac{c_4 h_A^2}{36 f_\pi^4 \pi^2} - \frac{c_4 g_A^2}{16 f_\pi^4 \pi^2} \tag{A13}$$

where $\tilde{b} = b_3 + b_8$.

[1] R. Machleidt and I. Slaus, J. Phys. G **27**, R69 (2001).
[2] S. R. Beane, P. F. Bedaque, K. Orginos, and M. J. Savage, Phys. Rev. Lett. **97**, 012001 (2006).
[3] N. Ishii, S. Aoki, and T. Hatsuda, Phys. Rev. Lett. **99**, 022001 (2007).
[4] R. Machleidt, K. Holinde, and C. Elster, Phys. Rep. **149**, 1 (1987).
[5] V. G. J. Stoks, R. A. M. Kompl, M. C. M. Rentmeester, and J. J. de Swart, Phys. Rev. C **48**, 792 (1993).
[6] V. G. J. Stoks, R. A. M. Klomp, C. P. F. Terheggen, and J. J. de Swart, Phys. Rev. C **49**, 2950 (1994).
[7] R. Machleidt, Phys. Rev. C **63**, 024001 (2001).
[8] S. Weinberg, Phys. Lett. **B251**, 288 (1990).
[9] C. Ordónez, L. Ray, and U. van Kolck, Phys. Rev. C **53**, 2086 (1996).
[10] P. F. Bedaque and U. van Kolck, Annu. Rev. Nucl. Part. Sci. **52**, 339 (2002).
[11] E. Epelbaum, Prog. Part. Nucl. Phys. **57**, 654 (2006).
[12] R. Machleidt and D. R. Entem, J. Phys. G **31**, S1235 (2005).
[13] N. Kaiser, R. Brockmann, and W. Weise, Nucl. Phys. **A625**, 758 (1997).
[14] N. Kaiser, S. Gerstendorfer, and W. Weise, Nucl. Phys. **A637**, 395 (1998).
[15] J. L. Friar, Phys. Rev. C **60**, 034002 (1999).
[16] M. C. M. Rentmeester, R. G. E. Timmermans, J. L. Friar, and J. J. de Swart, Phys. Rev. Lett. **82**, 4992 (1999).
[17] D. B. Kaplan, M. J. Savage, and M. B. Wise, Phys. Lett. **B424**, 390 (1998).
[18] D. B. Kaplan, M. J. Savage, and M. B. Wise, Nucl. Phys. **B534**, 329 (1998).
[19] S. R. Beane, P. F. Bedaque, M. J. Savage, and U. van Kolck, Nucl. Phys. **A700**, 377 (2002).
[20] T. Frederico, V. S. Timoteo, and L. Tomio, Nucl. Phys. **A653**, 209 (1999).
[21] S. R. Beane, D. B. Kaplan, and A. Vuorinen (2008), arXiv:0812.3938.
[22] D. R. Entem and R. Machleidt, Phys. Rev. C **66**, 014002 (2002).
[23] D. R. Entem and R. Machleidt, Phys. Lett. **B524**, 93 (2002).
[24] D. R. Entem and R. Machleidt, Phys. Rev. C **68**, 041001(R) (2003).
[25] E. Epelbaum, W. Glöckle, and U.-G. Meißner, Nucl. Phys. **A671**, 295 (2000).
[26] E. Epelbaum, W. Glöockle, and U.-G. Meißner, Eur. Phys. J. A **19**, 125 (2004).
[27] E. Epelbaum, W. Glöckle, and U.-G. Meißner, Eur. Phys. J. A **19**, 401 (2004).
[28] E. Epelbaum, W. Glöckle, and U.-G. Meißner, Nucl. Phys. **A747**, 362 (2005).
[29] M. Pavon Valderrama and E. Ruiz Arriola, Phys. Rev. C **72**, 054002 (2005).
[30] M. P. Valderrama and E. R. Arriola, Phys. Rev. C **74**, 054001 (2006).
[31] M. Pavon Valderrama and E. Ruiz Arriola, Phys. Rev. C **74**, 064004 (2006).
[32] A. Nogga, R. G. E. Timmermans, and U. van Kolck, Phys. Rev. C **72**, 054006 (2005).
[33] K. M. Case, Phys. Rev. **80**, 797 (1950).
[34] W. Frank, D. J. Land, and R. M. Spector, Rev. Mod. Phys. **43**, 36 (1971).

[35] E. Ruiz Arriola, A. Calle Cordon, and M. Pavon Valderrama (2007), arXiv:0710.2770 [nucl-th].
[36] M. Pavon Valderrama and E. R. Arriola, Ann. Phys. **323**, 1037 (2008).
[37] S. R. Beane, P. F. Bedaque, L. Childress, A. Kryjevski, J. McGuire, and U. van Kolck, Phys. Rev. A **64**, 042103 (2001).
[38] B. Long and U. van Kolck, Ann. Phys. **323**, 1304 (2008).
[39] C. J. Yang, C. Elster, and D. R. Phillips, Phys. Rev. C **77**, 014002 (2008).
[40] C. J. Yang, C. Elster, and D. R. Phillips (2009), arXiv:0901.2663.
[41] U. van Kolck, Nucl. Phys. **A645**, 273 (1999).
[42] D. R. Entem, E. Ruiz Arriola, M. Pavon Valderrama, and R. Machleidt, Phys. Rev. C **77**, 044006 (2008).
[43] M. P. Valderrama, A. Nogga, E. Ruiz Arriola, and D. R. Phillips, Eur. Phys. J. A **36**, 315 (2008).
[44] E. Epelbaum and U. G. Meißner (2006), nucl-th/0609037.
[45] M. C. Birse, Phys. Rev. C **74**, 014003 (2006).
[46] D. R. Entem, F. Fernandez, and A. Valcarce, Phys. Rev. C **62**, 034002 (2000).
[47] D. Bartz and F. Stancu, Phys. Rev. C **63**, 034001 (2001).
[48] A. Valcarce, H. Garcilazo, F. Fernandez, and P. Gonzalez, Rep. Prog. Phys. **68**, 965 (2005).
[49] M. Ademollo, G. Veneziano, and S. Weinberg, Phys. Rev. Lett. **22**, 83 (1969).
[50] E. Jenkins and A. V. Manohar, Phys. Lett. **B255**, 558 (1991).
[51] T. R. Hemmert, B. R. Holstein, and J. Kambor, J. Phys. G **24**, 1831 (1998).
[52] H. Krebs, E. Epelbaum, and U.-G. Meißner, Eur. Phys. J. A **32**, 127 (2007).
[53] T. E. O. Ericson and W. Weise, *Pions and Nuclei* (Oxford, 1988), Vol. 74, p. 479.
[54] G. Cattapan and L. S. Ferreira, Phys. Rep. **362**, 303 (2002).
[55] C. Ordónez and U. van Kolck, Phys. Lett. **B291**, 459 (1992).
[56] U. van. Kolck, Ph.D. thesis, Texas (1991).
[57] V. R. Pandharipande, D. R. Phillips, and U. van Kolck, Phys. Rev. C **71**, 064002 (2005).
[58] E. Epelbaum, H. Krebs, and U.-G. Meißner, Nucl. Phys. **A806**, 65 (2008).
[59] M. Pavon Valderrama and E. Ruiz Arriola, nucl-th/0605078.
[60] V. A. Baru *et al.*, Phys. Lett. **B659**, 184 (2008).
[61] S. Weinberg, Nucl. Phys. **B363**, 3 (1991).
[62] E. Matsinos, Phys. Rev. C **56**, 3014 (1997).
[63] N. L. Rodning and L. D. Knutson, Phys. Rev. C **41**, 898 (1990).
[64] V. G. J. Stoks, P. C. van Campen, W. Spit, and J. J. de Swart, Phys. Rev. Lett. **60**, 1932 (1988).
[65] J. Martorell, D. W. L. Sprung, and D. C. Zheng, Phys. Rev. C **51**, 1127 (1995).
[66] D. M. Bishop and L. M. Cheung, Phys. Rev. A **20**, 381 (1979).
[67] J. J. de Swart, C. P. F. Terheggen, and V. G. J. Stoks, nucl-th/9509032.
[68] M. Pavon Valderrama and E. Ruiz Arriola, Eur. Phys. J. A **31**, 549 (2007).
[69] D. R. Phillips, Phys. Lett. **B567**, 12 (2003).
[70] R. A. Gilman and F. Gross, J. Phys. G **28**, R37 (2002).
[71] R. Higa, M. Pavon Valderrama, and E. Ruiz Arriola, Phys. Rev. C **77**, 034003 (2008).
[72] N. Kaiser, Phys. Rev. C **61**, 014003 (1999).
[73] N. Kaiser, Phys. Rev. C **62**, 024001 (2000).
[74] N. Kaiser, Phys. Rev. C **63**, 044010 (2001).